

**OXIDATION AND THERMAL STABILITY
ENHANCEMENT OF EMULSIFIED PALM OIL
METHYL ESTER IN DIESEL ENGINE**

SYEDA REHAM SHAHED

**DISSERTATION SUBMITTED IN FULFILMENT OF THE
REQUIREMENTS FOR THE DEGREE OF MASTER OF
ENGINEERING SCIENCE**

**FACULTY OF ENGINEERING
UNIVERSITY OF MALAYA
KUALA LUMPUR**

2017

UNIVERSITY OF MALAYA

ORIGINAL LITERARY WORK DECLARATION

Name of Candidate: Syeda Reham Shahed

Matric No: KGA140006

Name of Degree: Master of Engineering Science

Title of Dissertation: Oxidation and thermal stability enhancement of emulsified palm oil methyl ester in diesel engine

Field of Study: Energy

I do solemnly and sincerely declare that:

- (1) I am the sole author/writer of this Work;
- (2) This Work is original;
- (3) Any use of any work in which copyright exists was done by way of fair dealing and for permitted purposes and any excerpt or extract from, or reference to or reproduction of any copyright work has been disclosed expressly and sufficiently and the title of the Work and its authorship have been acknowledged in this Work;
- (4) I do not have any actual knowledge nor do I ought reasonably to know that the making of this work constitutes an infringement of any copyright work;
- (5) I hereby assign all and every rights in the copyright to this Work to the University of Malaya ("UM"), who henceforth shall be owner of the copyright in this Work and that any reproduction or use in any form or by any means whatsoever is prohibited without the written consent of UM having been first had and obtained;
- (6) I am fully aware that if in the course of making this Work I have infringed any copyright whether intentionally or otherwise, I may be subject to legal action or any other action as may be determined by UM.

Candidate's Signature

Date:

Subscribed and solemnly declared before,

Witness's Signature

Date:

Name:

Designation:

ABSTRACT

Energy coming from fossil fuels are non-renewable, therefore, they have a negative effect on the environment namely- greenhouse effect or global warming. Researchers are conducting a lot of studies on renewable fuel to practice it as an alternative fuel for transportation and other uses. Biofuel has been widely accepted as a very potential renewable energy that can replace the conventional use of fossil fuel for diesel engine. Biodiesels can be used in conventional diesel engine without any modification and can also reduce harmful emissions. However, biodiesel have low oxidation stability which sometimes affect badly while storing and using it as fuel. This research is aimed to improve oxidation stability as well as thermal stability of biodiesel through emulsification process. In the emulsification process water is added to biodiesel with the help of surfactant (TritonX-100) and co-surfactant (ethanol) to make the mixture stable. FTIR (Fourier transform infrared spectroscopy) and proton NMR (Nuclear magnetic resonance) are used to analyze the chemical bond characteristics of biodiesel emulsion. Oxidation stability, thermal stability and lubrication characteristics of emulsified palm oil biodiesel is then investigated. It has been found that the oxidation stability of emulsified biodiesel is 102% higher than diesel and 27% higher than neat biodiesel. Thermo-gravimetric analysis shows improved thermal property of biodiesel emulsion compared to both diesel and neat biodiesel. The friction and wear test of emulsified biodiesel conducted with four ball tribo tester according to ASTM 4172 method (1200 rpm, 75°C temperature and 40 kg load). The improved lubricating performance found with emulsified biodiesel due to lower coefficient of friction and wear scar diameter compared to petroleum diesel fuel and neat biodiesel. In conclusion, addition of TritonX-100 and ethanol with small amount of water with biodiesel improves its oxidation and thermal stability and own improved lubricating characteristics compared to diesel and biodiesel fuel.

ABSTRAK

Tenaga yang berasal daripada bahan api fosil ialah tenaga yang tidak boleh diperbaharui, oleh itu, ia mempunyai kesan negatif terhadap alam sekitar iaitu - kesan rumah hijau atau pemanasan global. Para penyelidik menjalankan banyak kajian mengenai bahan api yang boleh diperbaharui untuk menggunakannya sebagai bahan api alternatif bagi pengangkutan dan kegunaan lain. Biobahan api telah diterima secara meluas sebagai tenaga yang boleh diperbaharui yang sangat berpotensi menggantikan penggunaan konvensional bahan api fosil untuk enjin diesel. Biodiesel boleh digunakan dalam enjin diesel konvensional tanpa sebarang pengubahsuaian dan juga boleh mengurangkan pelepasan yang berbahaya. Walau bagaimanapun, biodiesel mempunyai kestabilan pengoksidaan yang rendah, dimana kadangkala mendatangkan kesan teruk semasa menyimpan dan menggunakannya sebagai bahan bakar. Kajian ini bertujuan untuk meningkatkan kestabilan pengoksidaan serta kestabilan haba biodiesel melalui proses pengemulsian. Dalam proses pengemulsian, air ditambahkan ke dalam biodiesel dengan bantuan surfaktan (TritonX-100) dan surfaktan bersama (etanol) untuk menjadikan campuran stabil. FTIR (spektroskopi inframerah transformasi Fourier) dan proton NMR (resonans magnetik nuklear) digunakan untuk menganalisis ciri-ciri ikatan kimia emulsi biodiesel. Kestabilan pengoksidaan, kestabilan haba dan ciri-ciri pelinciran biodiesel minyak sawit yang diemulsi kemudian dikaji. Dapatan menunjukkan bahawa kestabilan pengoksidaan biodiesel yang diemulsi adalah 102% lebih tinggi daripada diesel dan 27% lebih tinggi daripada biodiesel asli. Analisis terma-gravimetrik menunjukkan peningkatan sifat haba untuk emulsi biodiesel berbanding dengan kedua-dua diesel dan biodiesel asli. Ujian geseran dan haus biodiesel yang diemulsi dijalankan dengan penguji tribo empat bola mengikut kaedah ASTM 4172 (kelajuan 1200 rpm, suhu 75 °C dan beban 40 kg). Peningkatan prestasi pelinciran yang didapati daripada biodiesel yang diemulsi disebabkan oleh pekali geseran dan diameter haus yang lebih rendah

berbanding bahan api diesel petroleum dan biodiesel asli. Kesimpulannya, penambahan TritonX-100 dan etanol dengan jumlah air yang kecil dengan biodiesel meningkatkan kestabilan pengoksidaan dan haba dan juga meningkatkan ciri-ciri pelinciran berbanding dengan diesel dan bahan bakar biodiesel.

University of Malaya

ACKNOWLEDGEMENT

I would like to thank almighty Allah s.w.t, the creator of the world for giving me the fortitude and aptitude to complete this thesis.

I would especially like to thank my supervisors Professor Ir. Dr. Masjuki Bin Haji Hassan and Associate Professor Dr. Md. Abul Kalam for their guidance, encourage and support throughout this work. I would like to express my gratitude to the Ministry of Higher Education (MOHE) for the financial support through High Impact Research (HIR) having grant no. UM.C/HIR/MOHE/ENG/60. Also, I would like to convey appreciation to all my colleagues at Centre for Energy Sciences (CFES) for their encouragement during my research work. Last but not the least, I am grateful to University of Malaya for preparing and giving opportunity to conduct this research.

University of Malaya

TABLE OF CONTENTS

ORIGINAL LITERARY WORK DECLARATION	ii
Abstract	ii
Abstrak	iii
Acknowledgement.....	v
Table of Contents	vi
List of Figures	ix
List of Tables.....	xi
List of Symbols and Abbreviations.....	xii
CHAPTER 1: INTRODUCTION.....	1
1.1 Background.....	1
1.1.1 Present and future energy scenario.....	1
1.1.2 Limitations of biofuel.....	2
1.1.3 Biodiesel emulsion	3
1.1.4 Problem statement	4
1.2 Objective.....	4
1.3 Scope of the study.....	4
1.4 Dissertation framework	6
CHAPTER 2: LITERATURE REVIEW.....	8
2.1 Introduction.....	8
2.2 Components and its preparation of emulsified biofuel.....	9
2.3 Stability of Biofuel emulsion.....	11
2.4 Comparative analysis physicochemical properties of tested biofuels	13
2.4.1 Density.....	16

2.4.2	Viscosity	17
2.4.3	Heating Value	19
2.4.4	Oxidation and thermal stability	20
2.5	Lubricating properties	21
2.6	Theory of tribology	22
2.6.1	Friction	22
2.6.2	Coefficient of friction (CoF)	23
2.6.3	Wear	23
2.6.3.1	Adhesive wear	25
2.6.3.2	Abrasive wear	25
2.6.3.3	Corrosive wear	25
2.6.3.4	Fatigue wear	26
CHAPTER 3: METHODOLOGY		27
3.1	Preparation of biodiesel emulsion and comparison of emulsifiers	27
3.2	Zetasizer	31
3.3	Optical microscope	32
3.4	Fuel properties measuring procedure and equipment	32
3.4.1	Density and viscosity measurement	33
3.4.2	Calorific value	35
3.4.3	Oxidation stability	37
3.5	FT-IR analysis	38
3.6	Proton NMR analysis	38
3.7	TGA and DSC analysis	39
3.8	Experimental setup and testing procedure of 4-ball tribo tester	41

CHAPTER 4: RESULTS AND DISCUSSION	43
4.1 Introduction.....	43
4.2 Physicochemical properties of emulsified palm oil methyl ester	43
4.3 Droplet distribution of biodiesel emulsion	44
4.4 Fourier transform infrared spectroscopy (FTIR) Analysis	47
4.4.1 Proton nuclear magnetic resonance (¹ H-NMR) analysis:.....	50
4.5 Thermogravimetric analysis (TGA)	55
4.6 Differential scanning calorimetry (DSC) analysis:.....	62
4.7 Friction and wear analysis.	65
4.7.1 CoF Analysis	65
4.7.2 Wear scar diameter analysis	68
4.7.3 SEM and EDX Analysis.....	70
4.7.4 Elemental analysis	72
CHAPTER 5: CONCLUSIONS AND RECOMMENDATION	74
5.1 Conclusion	74
5.2 Recommendation for future work.....	75
References	76
List of publications and papers presented	86
Appendix	87

LIST OF FIGURES

Figure 1.1: Chemical structure of surfactants used in the study	6
Figure 2.1: World palm oil production 2013 (Agriculture, 2013)	9
Figure 2.2: Variation of density with water concentration of different fuels (Reham et al., 2015)	17
Figure 2.3: Variation of kinematic viscosity with water concentration of different fuels (Reham et al., 2015)	18
Figure 2.4: Variation of heating value with water concentration of different fuels (Reham et al., 2015).....	20
Figure 2.5: Schematic diagram of different types of wear (Bhushan, 2000)	24
Figure 3.1: Emulsion preparation.....	28
Figure 3.2: Emulsion type identification test	30
Figure 3.3: Zetasizer equipment set up for droplet size measurement.....	31
Figure 3.4: Optical microscope used to visualize water droplet in emulsion	32
Figure 3.5: Viscometer.....	34
Figure 3.6: Calorimeter	35
Figure 3.7: Biodiesel Rancimat.....	37
Figure 3.8: FT-IR spectrometer	38
Figure 3.9: NMR spectrometer	39
Figure 3.10: Thermo-gravimetric analyser	40
Figure 3.11: DSC analyser	40
Figure 3.12: Schematic Diagram of 4 ball tribo tester	42
Figure 4.1: This shows the water droplet distribution of (a) MTX-1 (b) MTX-2 (c) MTX-3 through optical microscope.	45
Figure 4.2: This shows the water droplet distribution of (a) MTX-1 (b) MTX-2 (c) MTX-3 with Zeta sizer	46

Figure 4.3: (a) transmittance (%T) vs wave number (cm^{-1}) curve of B-100 and (b) transmittance (%T) vs wave number (cm^{-1}) curve of MTX-1, MTX-2 and MTX-3.	48
Figure 4.4: $^1\text{H-NMR}$ signals of MTX-1, surfactant and B-100 around chemical shift of 1.3 ppm.....	51
Figure 4.5: Chemical shift of B-100, MTX01, MTX-2 and MTX-3 in ppm.....	52
Figure 4.6: Onset and offset temperatures of (a) neat biodiesel and (b) MTX-1 biodiesel emulsion during thermal decomposition.....	56
Figure 4.7: Weight change with respect to temperature and derivative weight change with respect to temperature are provided for (a) Diesel, (b) B-100 (Palm biodiesel) (c) MTX-1, (d) MTX-2 and (e) MTX-3.	57
Figure 4.8: Derivative of weight change with respect to temperature vs time of neat biodiesel and emulsified biodiesel	61
Figure 4.9: Change of weight with respect to time vs temperature of B-100 and emulsified biodiesel samples.....	61
Figure 4.10: DSC curve analysis of Palm biodiesel at $10\text{ }^\circ\text{C min}^{-1}$ heating rate for (a) cooling scans (b) heating scans.	64
Figure 4.11: Friction co-efficient behaviour with respect to time in (a) run-in-period and (b) steady state condition	67
Figure 4.12: Average CoF value of samples during steady state condition.....	69
Figure 4.13: Wear scar diameter of different fuel samples.....	69
Figure 4.14: SEM analysis of the wear areas of steel ball	71
Figure 4.15: Element abundance in percentage at the wear surface of the steel ball for each sample	72

LIST OF TABLES

Table 2.1: Physicochemical properties of biofuels and their emulsions (Reham et al., 2015)	14
Table 2.2: Advantages and disadvantages of diesel and biodiesel emulsion.....	26
Table 3.1: Fuel property of Palm oil methyl ester (B-100).....	27
Table 3.2: Properties of emulsion prepared from three surfactants	29
Table 3.3: Information of the equipment used for fuel property measurement	33
Table 3.4: Technical data for Anton paar (SVM 3000) viscometer.....	35
Table 3.5: Technical data of calorimeter.....	36
Table 3.6: Technical data of Rancimat	38
Table 3.7: Composition of biodiesel-diesel blend.....	41
Table 3.8: Experimental operating conditions for four ball machine	42
Table 4.1: Fuel property of emulsified biodiesel	44
Table 4.2: FTIR results of B-100, MTX-1, MTX-2, and MTX-3.....	49
Table 4.3: ¹ H-NMR analysis of Surfactant.....	53
Table 4.4: ¹ H-NMR analysis of B-100.....	53
Table 4.5: ¹ H-NMR analysis of biodiesel emulsion	54
Table 4.7: Thermal characteristics (DSC) of neat and emulsified palm biodiesels	63

LIST OF SYMBOLS AND ABBREVIATIONS

ASTM	:	American Society of Testing Materials
B-100	:	Neat Palm Biodiesel
CoF	:	Coefficient of friction
CV	:	Calorific value (J/g)
ρ	:	Density (kg/m ³)
d	:	Doublet
DSC	:	Differential scanning calorimetry
EDX	:	Energy dispersive X-Ray
FAME	:	Fatty acid methyl esters
FT-IR	:	Fourier transform infrared spectroscopy
HLB	:	Hydrophilic-lipophilic balance
NMR	:	Nuclear magnetic resonance
q	:	Quartet
s	:	Singlet
SEM	:	Scanning electron microscope
t	:	Triplet
TGA	:	Thermal gravimetric analysis
W/O	:	Water in oil two phase emulsion
O/W/O	:	Oil in water in oil three phase emulsion
WSD	:	Wear scar diameter
% wt	:	Weight change in percentage

CHAPTER 1: INTRODUCTION

1.1 Background

Modern civilization is very much dependent on non-renewable fossil resources like coal, petroleum and natural gas. In recent years, ever increasing trend of energy consumption due to industrialization and development has caused serious threat to the energy security and environment. Global fossil fuel consumption grew 0.6 million barrels per day and cost \$ 111.26 per barrel in 2011 which means a 40% increase than 2010 level (Petroleum, 2011). Global oil consumption increased 0.8%, natural gas and coal consumption increased 0.4% each in 2014 (IER, 2015). Current reserve of liquid fuel has the capacity to meet only half of the usual energy demand until 2023 (Owen et al., 2010). Besides, this tremendous drift of fossil fuel use, hazardously effecting world's environment, which includes global warming, deforestation, eutrophication, ozone depletion, photochemical smog and acidification (Armas et al., 2006).

1.1.1 Present and future energy scenario

Major portion of the petroleum and natural gas reserve is distributed within a small region of the world. Middle East countries are the dominant petroleum suppliers and possess 53% of global petroleum reserve (OPEC, 2016). On contrary, Renewable energy sources are more evenly distributed than fossil fuel and hence, coming up as a secured energy source in near future (Demirbas, 2009a). Greater energy security, reducing environment pollution, saving foreign exchange and other socio-economic issues stimulating rapid growth of biofuel industries over the next decade (Demirbas, 2009b). Staniford demonstrated a projection back in 2008 on global marketed primary energy production from 1970 to 2050 which strongly supports the increasing trend of renewable energy consumption (Staniford, 2008). In a reference case, showed by EIA, renewable energy possessed 10% share of the total energy used in 2008 and it will be increased to

14% in 2035. They mentioned it as world's fastest growing form of energy ((IEA), 2011). Biodiesel is progressively gaining acceptance as an alternative and renewable energy source and market demand will rise intensely in near future (Basha et al., 2009; Foo & Hameed, 2009; Janaun & Ellis, 2010). According to International Energy Agency (IEA), around 27% of total transport fuel will be replaced completely by biofuels within 2050 (IEA, 2011).

1.1.2 Limitations of biofuel

Massive increase in fuel production from edible feedstock has raised a highly controversial "food vs. fuel" debate which is not new in the international agenda (Kuchler & Linnér, 2012). In present situation, more than 95% of biofuel is produced from edible oil source (Kuchler & Linnér, 2012). Rapeseed, palm, sunflower and soybean are the main edible sources of biofuel industry (Wang et al., 2012). Use of edible feedstock for producing biofuel puts threat on food security and cultivable land which has been criticized by many environmentalists worldwide. Besides, biofuel feedstock is expensive than diesel fuel. Cost of biofuel feedstock comprises around 70% of the total expenditure involved in the production process. Thus, minimizing the cost of biofuel feedstock has been the one of the requirements for most biofuel producers around the globe (Phan & Phan, 2008). Even though use of non-edible feedstock for biodiesel production minimizes the lowers threat on food security, but improved emission is highly desirable for its application. Biofuels are considered an economically feasible option as alternate fuel because of their improved emission characteristics. Although burning of biodiesel results in reduced emissions of carbon monoxide (CO), total hydrocarbon (THC), particulate matter (PM), and polyaromatic hydrocarbons (PAH), the emission of nitrogen oxides (NO_x) is high because of higher oxygen content in biodiesel (Hoekman & Robbins, 2012; Özcanlı et al., 2011; Rizwanul Fattah et al., 2014; Rizwanul Fattah et al., 2013; Xue et al., 2011). Use of biodiesel and its blends in CI engine results in loss of

torque, power, and also increased in brake specific fuel consumption was reported by researchers (Dhar et al., 2012; Khond & Kriplani, 2016). Therefore, demand for reduced energy use and reduction of environment pollution keeping engine performance unaltered became a challenge for researchers.

1.1.3 Biodiesel emulsion

Recent advancement in biodiesel promotes emulsification of fuel to reduce energy consumption and emissions from diesel engines. Fuel emulsification is considered one of the techniques of introducing water to the combustion chamber to reduce the emissions of NO_x, smoke, and particulate matter (PM) (Abu-Zaid, 2004; Atmanlı et al., 2014; Crookes et al., 1997; Debnath et al., 2013; Koc & Abdullah, 2013; Labeckas et al., 2014; Lif & Holmberg, 2006; Lin & Wang, 2003; Lin & Lin, 2011; Palash et al., 2013). A recent experimental use of emulsified fuel in ferry has been done in New Zealand (Motorship, 2014). About 5% fuel was saved at high loads and notable reduction in NO_x and particulate emission. Emulsification provides greater atomization of fuel through vaporization of water and promotes more complete combustion. Cooler environment due to water vaporization supported significantly lower NO_x emission. In automotive, emulsified fuel also proved to have better fuel characteristics compared to biodiesel and diesel. Prakash et al. (Prakash et al., 2015) found 35% lower HC emission in emulsified Jatropha methyl ester (JME) compared to that of JME alone. Therefore, emulsification of biodiesel is a potential research area to minimize the limitation on use of biodiesel alone. Though many studies been carried out in engine performance and combustion, few researches is been carried out in oxidation and thermal stability of biodiesel emulsion. Therefore, aim of this study is to improve the oxidation and thermal stability of biodiesel through emulsification.

1.1.4 Problem statement

Storage of biodiesel for commercial usage is restricted due to poor oxidation stability (Knothe, 2007). Presence of saturated bonds in biodiesel make it more vulnerable to oxidation than diesel. Instability is proportional to the amount of unsaturated fatty acids present in the molecules (Knothe, 2007). Therefore, physical and chemical characteristics of biodiesel changes due to oxidation. The oxidation causes wear and corrosion in engine. To improve oxidation stability anti-oxidants are used. However, due to high cost use of anti-oxidants are not always feasible. Therefore, aim of this study is to improve oxidation stability through emulsion. Novelty of the study is to improve oxidation stability by emulsifying biodiesel with water.

1.2 Objective

The objectives of this study are as follows:

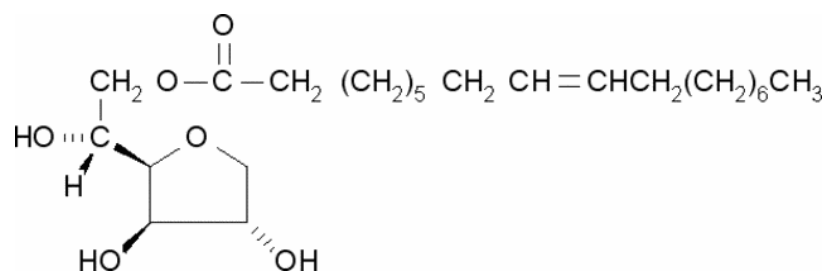
- To characterize the physicochemical properties of emulsified biodiesel
- To investigate the effect of emulsification on oxidation stability and thermal stability of palm biodiesel
- To analyze the lubricating characteristics of emulsified biodiesel

1.3 Scope of the study

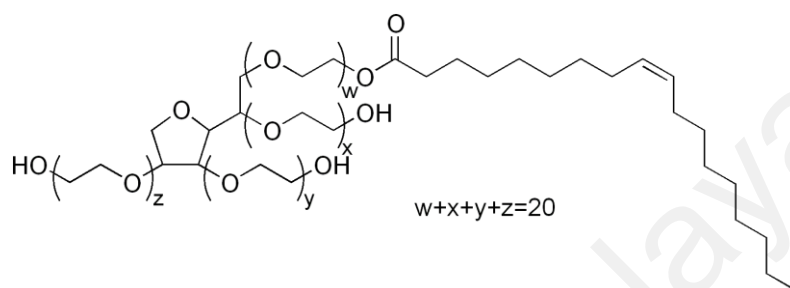
Palm methyl ester is used as base oil. Palms are most popular and most extensively cultivated amongst the plant families. Around 202 genera and approximately 2600 species of palms are currently known and available mostly at tropical, subtropical and climates where weather is warm. Worlds total palm oil production is 45 million tons per year and about 87% of world palm oil production is contributed by Malaysia, Indonesia and Thailand (Plantation, 2014). Due to its massive usage, this feedstock is taken as testing purpose and aim of the study is to improve its fuel properties through emulsification. This study primarily analyses three areas of emulsified biodiesel- the physicochemical

properties and bond characteristics, thermal stability and lastly lubrication characteristics with wear analysis. Scope of the study is as follows:

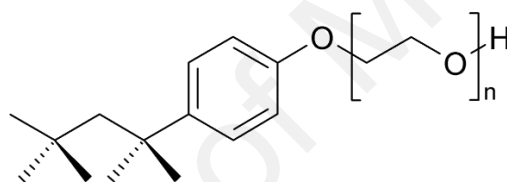
- To prepare the emulsion three different emulsifiers are used; namely- Span 80, Tween 80 and Triton-X -100. **Figure 1.1** shows the chemical structures of surfactants. As co-surfactant ethanol is used. Different concentrations of water are used for preparation of biodiesel emulsion. For fuel property tests – density, viscosity, calorific value, and oxidation stability etc. were performed. Though more parameters may consider for better analysis. Due lack of equipment facility some tests were not possible to conduct.
- To analyze the functional groups of molecules- Proton-NMR and FTIR analysis were performed. To explore thermal stability thermogravimetric analysis were performed.
- Lastly, to explore the wear and friction characteristics 4-ball tribo test was performed. Data from all the tests analysis is reported and a conclusion is made based on all findings.



(a) Span80



(b) Tween80



(c) TritonX-100

Figure 1.1: Chemical structure of surfactants used in the study

1.4 Dissertation framework

This dissertation is framed with five chapters. Summary of each chapter is listed as follows:

Chapter 1 briefed about energy situation worldwide and the problems associated with energy which further rolls in to solving problems by discussing different research topics. The chapter discussed on the present energy crisis and how it can be solved by using renewable energy sources, like – biofuel. Then it summarizes the importance and limitation of biodiesel. After that, it discussed importance of biodiesel emulsion to

mitigate the disadvantages of biodiesel. Finally, the objectives and scope of the study were discussed.

Chapter 2 summarizes the preparation of biodiesel emulsion along with its stability and physicochemical properties. Then the oxidation and thermal stability of biodiesel were discussed. Followed by, lubrication characteristics of biodiesel were discussed and types of wear that occurs in diesel engine were briefed with illustration.

Chapter 3 provides description of all the materials and equipment used to attain the objectives of this study.

Chapter 4 explains elaborately the results found in the experiments which were carried out in this study. This chapter also provides results in illustrations, graphical image and tabulated form. Each results comes with analysis and discussion.

Chapter 5 provides a summary of the major findings in this study along with recommendation for future studies.

CHAPTER 2: LITERATURE REVIEW

2.1 Introduction

In the economic development of any country, diesel fuel plays a significant role. It is widely used in agricultural, transportation and construction sectors etc. As a result, demand of diesel fuel is increasing rapidly. However, diesel fuel is considered to be one of the major contributors to environmental pollution. Diesel fuel contains 20-24% aromatics, such as benzene, toluene, xylenes etc. These compounds are volatile and toxic, and are responsible for fire/health hazards and environmental pollution (Çaynak et al., 2009). Moreover, global primary fuel consumption in 2010 is almost double of that in 1980 (Ong et al., 2011). Therefore, as the demand increasing rapidly, the reservations of fossil fuel rapidly decreasing and resulting in rise in oil prices every day (Jaichandar & Annamalai, 2013; Tesfa et al., 2012). For these reasons, researchers are emphasizing on searching for alternative clean fuels which are economically competitive, technically feasible, readily available and environmentally acceptable (Khatri et al., 2010). In recent years, biodiesel and its derivatives, have received attention as a suitable alternative for diesel fuel. Implication of vegetable oil in internal combustion engine dates back to Dr. Rudolf Diesel's development of diesel engine. In 1890, he used peanut oil as a fuel to exhibit his invention. The striking features of biodiesel are non-toxic emissions, excellent lubricity, bio-degradability, renewability, high cetane number, absence of sulfur and aromatic compounds (Anand et al., 2011; Atadashi et al., 2012).

Palms are most popular and most extensively cultivated amongst the plant families. Around 202 genera and approximately 2600 species of palms are currently known and available mostly at tropical, subtropical and climates where weather is warm. Basically, oil palm tree is originated from West Africa where it was growing wild and human started using palm oil 5000 years ago, later cultivation started mostly in all tropical areas of the

world considering its economic aspects. World's total palm oil production is 45 million tonnes per year and maximum production is in South East Asia. As shown in **Figure 2.1** about 87% of world palm oil production is contributed by Malaysia, Indonesia and Thailand. From 1990 to 2013 palm crop plantation area increased from 2.03 to 4.49 million hectares in Malaysia which means an increase of 121.2% (Agriculture, 2013; United States Department of Agriculture, 2007).

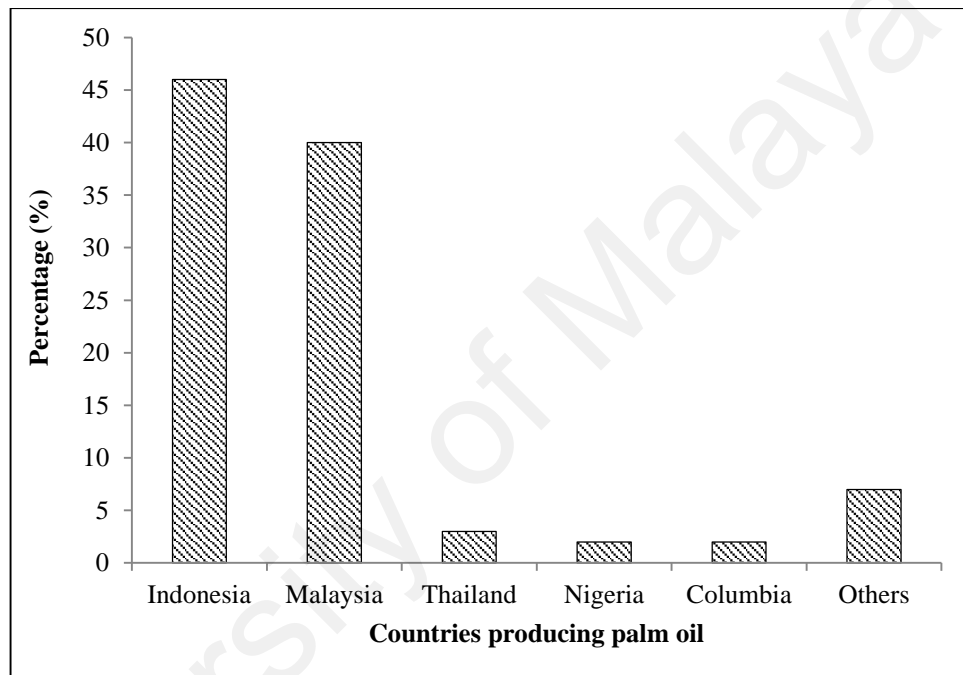


Figure 2.1: World palm oil production 2013 (Agriculture, 2013)

2.2 Components and its preparation of emulsified biofuel

An emulsion is a mixture of two or more immiscible liquids (Hans-Jurgen Butt, 2013; Ithnin et al., 2014). In the mixture, one of the liquids exists in dispersed droplets and the other is in continuous phase. Dispersed droplets throughout the mixture are referred to as internal phase, and the other one is termed as external phase (Alahmer et al., 2010; Ithnin et al., 2014; Nadeem et al., 2006). Emulsified fuels are emulsions composed of water and a combustible liquid (i.e., fuel), in which water is in the form of dispersed droplets (Moser, 2011). As oil and water are inherently immiscible with each other, a surfactant/emulsifier is used to prepare emulsion (Lin & Chen, 2006; Lin & Wang, 2003).

Many research has been conducted in diesel emulsion and analyzed its combustion, performance and emission (Ithnin et al., 2014, Alhamer et al., 2010; Kjong et al., 2016). But few is been conducted in biodiesel emulsion.

A surfactant molecule has two parts: one has affinity for water and the other has affinity for oil. The emulsifying agent or surfactant forms a thin interfacial film between the two liquids to decrease water surface tension and minimize the contact, coalescence, and aggregation of the internal dispersed phase (Chen & Tao, 2005; Friberg et al., 1995; Moilanen et al., 2009). Surfactants work spontaneously and aggregate in water to form well-defined structures called association colloids (Hans-Jurgen Butt, 2013). The HLB of a surfactant is a measure of the degree to which it is hydrophilic or lipophilic, and it is determined by calculating values for the different regions of the molecule. Surfactants are classified according to their HLB value, which affects their usage. An optimal value of HLB is necessary for the stabilization of emulsion (Griffin, 1949a). In general, surfactant molecules with low HLB, such as sorbitan ester, polyglycerol polyricinoleate, and soy lecithin, are used for water in oil (W/O) emulsions (Ambrosone et al., 2007; Gülseren & Corredig, 2014; Nesterenko et al., 2014; Porras et al., 2008; Züge et al., 2013). Koc et al. (Koc & Abdullah, 2013) used an anionic surfactant (dioctyl sodium sulfosuccinate) with 98% purity and 10.2 HLB. The selection of such an anionic surfactant is for HLB balance and can be used without a co-surfactant (Koc & Abdullah, 2013). Low HLB values of 4–6 are used to produce W/O emulsion, (Debnath et al., 2013; Griffin, 1949b; Hagos et al., 2011; Ithnin et al., 2014; Nadeem et al., 2006; Ushikubo & Cunha, 2014), and higher HLB values of 8–18 are used for oil in water (O/W) emulsions (Debnath et al., 2013; Griffin, 1949b).

Emulsified biodiesel can be two-phase (W/O) and three-phase emulsion (oil in water in oil (O/W/O). To produce water in biodiesel emulsion, the base oil is mixed with

lipophilic surfactant, added with water, and evenly stirred via an electromagnetic stirring machine (Debnath et al., 2013). If the surfactant is hydrophilic, it is mixed with water instead of base fuel. The mixture can be prepared using mechanical, electronic, magnetic, or ultrasonic forces (Koc & Abdullah, 2013; Senthil, 2009). Micro emulsions are formed instantaneously when all components are combined in required proportions and usually do not need strong stirring or agitation. (Fernando & Hanna, 2005; Matthews et al., 2010). Volume fraction of surfactant is generally significant in micro emulsion (Hans-Jurgen Butt, 2013). Surfactants form semi-flexible elastic films at the interface, and the interfacial tension of micro emulsions is very small (Hans-Jurgen, 2013). Generally, the three-phase emulsion is prepared using two-stage emulsification method (Laugel et al., 1998; Lin & Lin, 2007). First, the O/W emulsion is prepared, and an emulsifying and homogenizing machine is then used to stir the biodiesel/surfactant mixture and simultaneously feed the O/W emulsion at a certain rate (Lin & Lin, 2007).

2.3 Stability of Biofuel emulsion

Stability of emulsified fuel is one of the prime concerns to make it commercially usable. Engine failure may occur if emulsified fuel is destabilized during storage or engine operation. Durability of this miscible state is a challenging issue. The destabilization of emulsion depends on temperature, amount of surfactant, viscosity, specific gravity, and water content (Clausse et al., 1999; Ithnin et al., 2014; Nadeem et al., 2006; Nesterenko et al., 2014; Opawale & Burgess, 1998). Water can co-exist with oil in four different states. Depending on these states, the characteristics of the emulsion also vary. The four states are stable, mesostable, unstable, and entrained water (Fingas & Fieldhouse, 2003). Some emulsions are highly stable and can be stored for several months. The viscosity and elasticity of such emulsions increase over time to at least three orders of magnitude higher than those of starting oil. Mesostable emulsions possess the properties between the stable and unstable emulsions. These emulsions are suspected to

have less sufficient stabilizing materials than destabilizing materials. These emulsions may degrade to form layers of oil and stable emulsions (Fingas & Fieldhouse, 2003). Unstable emulsion decomposes to oil and water rapidly after mixing within a few hours. The viscosity of unstable oil emulsion is less than that of net oil (Fingas & Fieldhouse, 2003). Thus, viscosity may become an indicator of emulsion stability.

Stability test method: Stability can be measured in two ways: 1) gravitational and 2) centrifugal stability tests. Gravitational stability test is conducted by bottle test method (Nesterenko et al., 2014; Porras et al., 2008). The sample is kept in a closed bottle in a fixed temperature region. At regular time intervals, the phase separation of the sample is monitored visually (Nesterenko et al., 2014). The least separated sample is considered more stable. The second method is the centrifugal stability test (Denkov et al., 2002; Lin & Lin, 2007). Lin & Lin (2007) observed the stability of emulsified biodiesel using centrifugal stability test. The fuel samples were centrifuged at 3000 rpm for 5 min, and the test tubes were kept motionless to observe the volume changes of the emulsion layer in their study. The least separated sample is accepted to have better stability. The centrifugal test is more suitable than the gravitational test method because the former is relatively simple and can be completed within a shorter time period (Denkov et al., 2002).

Surfactant plays a key role in the formation of biofuel emulsion. Therefore, the type of surfactant and its concentration play an important role in the stability of emulsion. The type of emulsifier may vary depending on the base fuel. In that case, the emulsifier with optimal performance should be used for the preparation of emulsion. Roila Awang & May (2008) used seven potential emulsifiers and screened out the best one. The amount of surfactant to be used during emulsion has a specific range as it strongly influences emulsion stability (Chen & Tao, 2005). At low concentrations of surfactants, emulsions are unstable because of oil droplet agglomeration. By contrast, at high concentrations,

rapid coalescence occurs and destabilizes the mixture because of polydispersity of surfactant micelles formed at the W/O interface as explained by Wasa et al. (2004). Thus, the emulsion is best stabilized at an optimal level of surfactant concentration. This range may vary with the base biofuel used for the emulsion. Kerihuel et al. (2005) kept their surfactant dosage within 2% to 8% to achieve stable emulsion using animal fat as base fuel. For palm oil emulsion, the highest stability is found at 1%–2% surfactant concentration (Roila Awang & May, 2008).

2.4 Comparative analysis physicochemical properties of tested biofuels

Table 2.1 shows the physicochemical properties of different biofuel emulsions. Among these 93% JME + 2% surfactant + 5% water + 100 ppm CNT (JME100CNT) emulsion possesses better physicochemical properties. The flash point of JME biodiesel is higher than that of diesel fuel, and the emulsified JME biodiesel with 5% water addition has an even higher flash point, which is an advantage (Sadhik Basha & Anand, 2014). However, Kannan & Anand (2011) found a much-reduced flash point for emulsified waste cooking oil with 0.5% water addition. The lower flash point is due to the addition of 19% (v/v) ethanol. As ethanol is highly flammable, its presence in fuel strongly affects its flash point. Hence, the use of ethanol is restricted when considering the fuel properties. The cetane number is higher in the case of emulsified fuel. Though micro emulsions have better stability than other types of emulsions, their calorific value is poor compared with that of other emulsions. Two-phase emulsion of soybean oil biodiesel possesses better properties compared with other types (Lin & Lin, 2007). **Figures 8 to 10** show the changes in properties of different fuels, for example JB10 (Raheman & Kumari, 2014), POME (Husnawan et al., 2009), soybean oil (Koc & Abdullah, 2013), *Thevetia peruviana* (Kannan & Gounder, 2011) and canola oil (Bhimani et al., 2013) with the variation in water concentration from different research studies. The observations of other properties from each of the graphs are stated below in corresponding sub-sections.

Table 2.1: Physicochemical properties of biofuels and their emulsions (Reham et al., 2015)

Fuel composition (% v/v)	Type of emulsion	Density kg/m ³	Heating value kJ/kg	Cetane number	Viscosity mm ² /s	Flash point °C	Ref.
Diesel		840	42490	45	4.59	52-96	(Senthil & Jaikumar, 2014)
Crude Jatropa Oil		899	36530		33.10	252	(Raheman & Kumari, 2014)
JME (Jatropa Methyl Ester)		895	38880	53	5.05	85	(Sadhik & Anand, 2014)
JME (Jatropa Methyl Ester)		895	38880	53	5.05	85	(Sadhik & Anand, 2014)
93% JME + 2% surfactant + 5% water	W/O	899.8	37050	51	5.40	140	
93% JME + 2% surfactant + 5% water + 25 ppm CNT (carbon nano tube)(JME25CNT)		897.2	37280	54	5.43	130	
93% JME + 2% surfactant + 5% water + 50 ppm CNT (JME50CNT)		897.8	37350	55	5.76	125	
93% JME + 2% surfactant + 5% water + 100 ppm CNT (JME100CNT)		899.4	37850	56	5.91	122	
JB10 (10% Jatropa biodiesel and 90% diesel)		837	40850		2.91	62	
JB10 +0.5% surfactant (HLB 5) + 10% Water		858	38720		3.93	68	(Raheman & Kumari, 2014)
POME (Palm oil methyl ester)		870	41700	51	4.7	121	(Husnawan et al., 2009)

Table 2.1: Continued.

Fuel composition (% v/v)	Type of emulsion	Density kg/m ³	Heating value kJ/kg	Cetane number	Viscosity mm ² /s	Flash point °C	Ref.
POME + 5% surfactant + 5% Water	W/O	890	37880	-	-	-	(Debnath et al., 2013)
Soybean Oil		864	40557	-	4.25	-	(Lin & in, 2007)
Soybean Biodiesel + 10% water	W/O	880	39669	-	7.29	-	(Lin & Lin, 2007)
	O/W/O	888	39219	-	7.66	-	(Lin & Lin, 2007)
Soybean Biodiesel + 10% water + 5% aqueous ammonia	O/W/O	885	39624	-	6.97	-	(Lin & Lin, 2007)
Soybean Oil + 20% Ethanol + 0.5% Water	Micro-emulsion	854.5	31294	-	-	-	(Matthews et al., 2010)
Soybean Oil + 20% Ethanol + 1% Water		855.2	31283	-	-	-	
Canola oil		960	40173	-	57.29	-	(Bhimani et al., 2013)
Canola oil + 9.8% methanol + 1.8% surfactant (Span 80 and Tween 80) HLB 7	W/O (Methanol in Oil)	900	38396	-	43.11	-	
Biodiesel produced from seed oil of <i>Thevetia peruviana</i> (TP)		860	41032	-	6.0	160	(Kannan & Gounder, 2011)
TP + 5% Water	W/O	867	38665	-	-	-	
Waste Cooking Palm oil (B70) + 0.5% water (approx.)	Micro-emulsion	841.98	37950	-	3.52	16.5	(Kannan & Anand, 2011)

2.4.1 Density

Majority of emulsified fuel has a larger density than the base fuel and diesel fuel itself because of the presence of water droplets in fuel (Debnath et al., 2013; Raheman & Kumari, 2014). Water addition of 5% increases density by 0.54% (Sadhik Basha & Anand, 2014), 2.3% (Debnath et al., 2013), and 0.8% for emulsified JME, POME, and emulsified TP, respectively. However, if alcohol is used for emulsion, the density will decrease (Bhimani et al., 2013). Canola oil is been emulsified with alcohol instead of water. Therefore, density of canola oil emulsion decreases with increase in methanol. Another study showed that three-phase emulsions have higher density than two-phase emulsions (Lin & Lin, 2007). Therefore, the extent of variation in density depends not only on the water but also on the base fuel, type of emulsion, and presence of alcohol. Higher density makes the fuel heavy and increases viscosity which is undesirable as it increases frictional forces. Frictional forces delays fuel flow and sometimes clogs the pipe, injector etc.

Density changes with the change in water concentration. This is illustrated in **Figure**

2.2. From **Figure 2.2** following observation can be made

- Density is increased when water concentration is increased
- Density is increased when methane concentration is increased for Canola oil. For emulsion of canola biodiesel methane was used instead of water.
- In the case of POME, the rate of increase is much higher than the rest between 10 to 15% water concentraion.
- JB 10, TP and Soybean oil give similar increasing trend and also offers a linear relationship with the concentraion of water

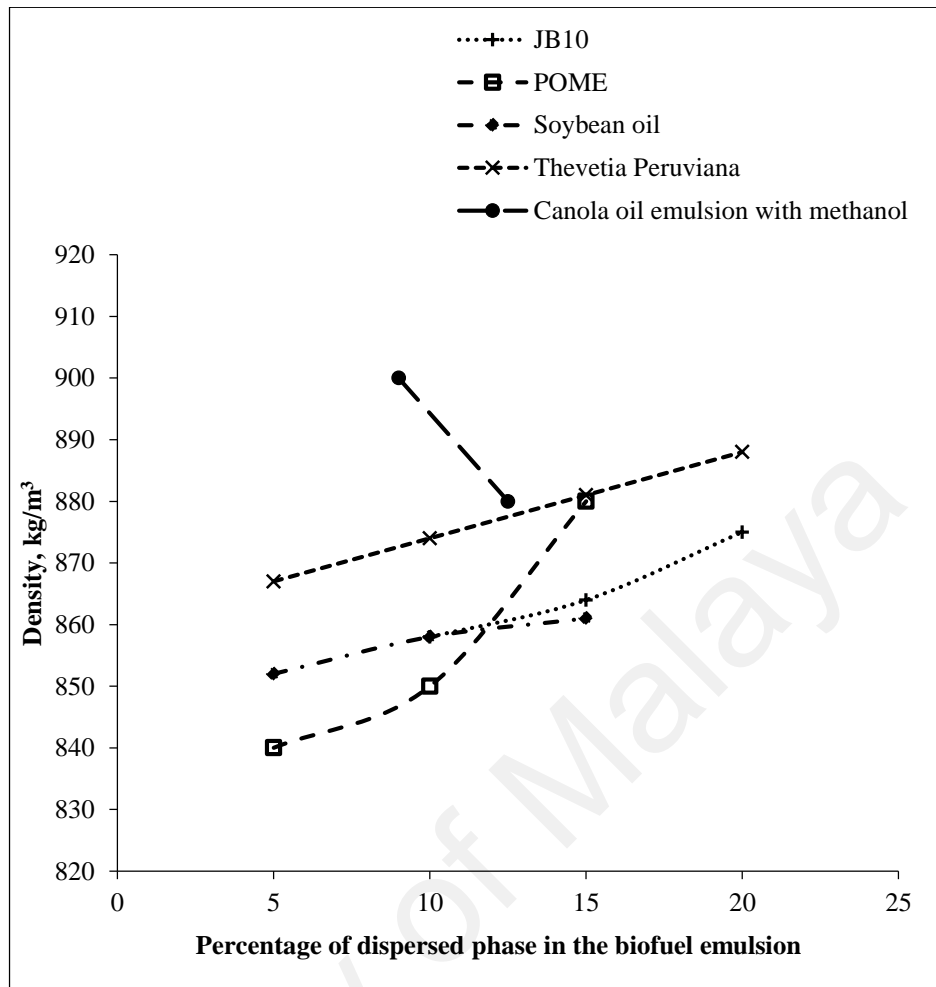


Figure 2.2: Variation of density with water concentration of different fuels (Reham et al., 2015)

2.4.2 Viscosity

Viscosity is one of the significant properties of fuel because it controls fuel injection characteristics, quality of atomization, and combustion. Large kinematic viscosities are found in emulsified soybean oil in three-phase emulsions, but the largest values are found in canola oil. Even though the viscosity is slightly larger than that of diesel, the engine encounters no problem during the operation for three-phase emulsions (Lin & Lin, 2008).

Table 2.1 shows that the viscosity of emulsified fuel increases because of the water content in the dispersed phase of water-emulsified biofuel (Lin & Lin, 2008). Emulsifying with 10% water increases viscosity by 35%, 71%, 80%, and 64% for JB10, two-phase emulsion of soybean biodiesel, three-phase emulsion of soybean biodiesel, and three-phase emulsion, respectively, with the addition of aqueous ammonia of soybean biodiesel.

However, alcohol can be used to reduce viscosity for emulsion purposes. According to the authors, the viscosity of methanol-emulsified canola biodiesel decreases by 24% (Bhimani et al., 2013). High viscosity of animal fats is also reduced using methanol (Kerihuel et al., 2005).

Viscosity changes with the change in water concentration. This is illustrated in **Figure 2.2**. From **Figure 2.2** following observation can be made

- The viscosity is almost constant with a minor variation with the increase in water for all except Canola oil
- Canola oil has highest viscosity and the increasing rate is also a bit higher than the rest

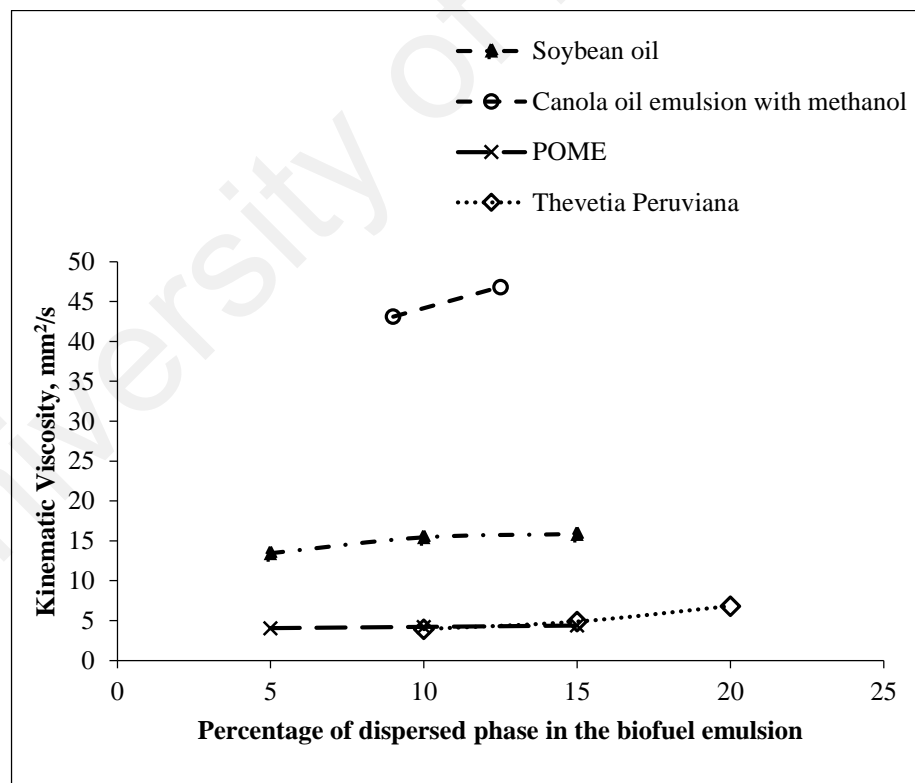


Figure 2.3: Variation of kinematic viscosity with water concentration of different fuels (Reham et al., 2015)

2.4.3 Heating Value

The calorific value of emulsified fuel is less than that of the base fuel (Bhimani et al., 2013; Debnath et al., 2013; Lin & Lin, 2007; Sadhik Basha & Anand, 2014) because of the increase in water content in the fuel. The water content is vaporized during combustion, taking up the heat generated in the combustion chamber and lowering the calorific value of fuel. Kannan & Anand (2011) limited water addition between 0.5 and 2 ml because of the reduction in lower heating value. **Table 2.1** shows that the addition of the same amount of water (10%) for emulsion results in a two-phase emulsion with a higher calorific value than the three-phase emulsion. With the same base oil (soybean biodiesel), Qi et al. (2010) and Matthews et al. (2010) found very low heating value with 0.5% water addition compared with that found by Lin et al. (2007) with 10% water addition. The poorer heating value can be explained by the addition of a large amount of ethanol because ethanol has a lower energy content. Koc & Abdullah (2013) found the heating value of biodiesel was around 10% less than the diesel fuel on weight basis. However, the calorific value can be increased using some additives, such as carbon nanotube (CNT) (Sadhik Basha & Anand, 2014) or aqueous ammonia for emulsion (Lin & Lin, 2007). By adding CNT up to 100 ppm, the heating value may increase by 2% (Sadhik Basha & Anand, 2014).

Heating value changes with the change in water concentration. This is illustrated in **Figure 2.4**. From **Figure 2.4** following observation can be made

- The variation of heating value gives a decreasing trend with the increase in water content
- The decreasing rate is slightly higher in the case of emulsified POME.
- JB10 and Soybean oil give similar decreasing trend

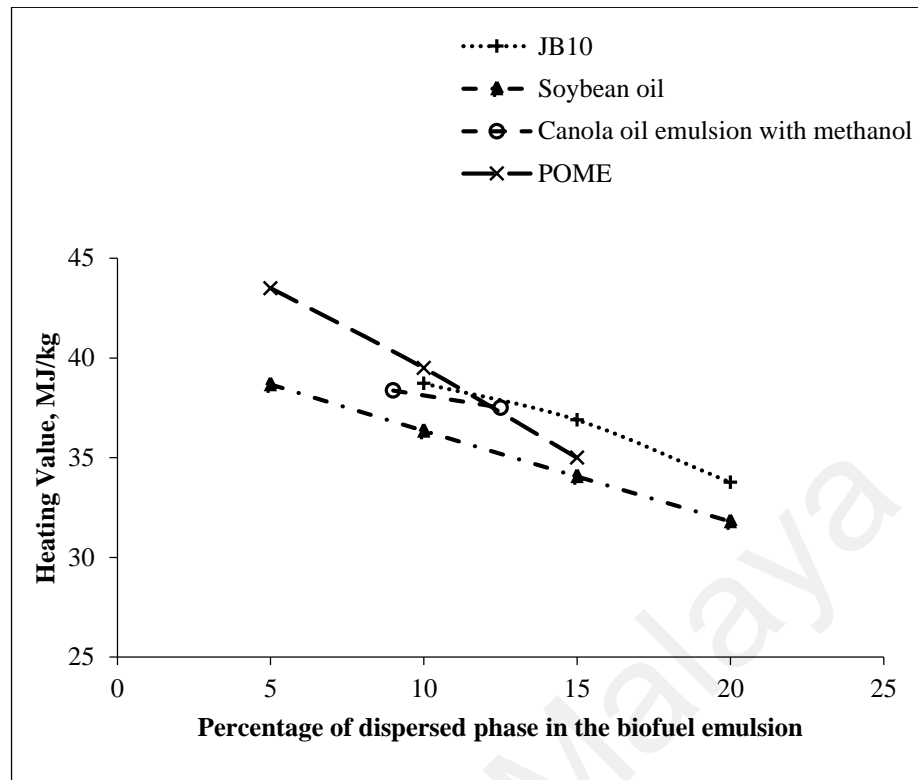


Figure 2.4: Variation of heating value with water concentration of different fuels (Reham et al., 2015)

2.4.4 Oxidation and thermal stability

Transesterification of oil or fats with small chain alcohol produces mono-alkyl esters known as biodiesel. However, the produced biodiesel has the same fatty acids composition like that of parent oil with high amount of unsaturated fatty acids. The presence of these unsaturated fatty acid make biodiesel sensitive to oxidation. Low oxidation stability of biodiesel leads to long term storage problems. Oxidation instability forms gums, sediment and darkens the fuel which is highly undesirable in engine operation. Biodiesel produce free radicals which reacts with oxygen and then produce free radicals in the molecular chain. When it react with olefinic compounds to form gums. Oxidation of fuel also changes the physicochemical properties, like – density, viscosity, acid value etc. (Jain & Sharma, 2010). Therefore use of anti-oxidant enhances its stability and can be stored for longer time (Joshi et al., 2013). Many research studies has been done on using efficient anti-oxidants (Balaji & Cheralathan, 2014; Palash et al., 2014,

İleri and Koçar, 2013). Palash et al., (2014) analysed the effect of antioxidant in four stroke multi cylinder engine using *Jatropha* biodiesel-diesel blend as fuel. They found the anti-oxidant reduced the NO_x emission. İleri and Koçar, (2013) studied engine performance and emission using four different antioxidants. They used canola methyl ester as biodiesel.

Besides, high temperature exposition, presence of metallic elements and ultraviolet radiation reduce the overall stability of biofuel. Biodiesel while used in engine, it is subjected to high temperature during combustion. Therefore, biofuel becomes prone to deterioration and forms deposits and insoluble in the fuel which leads to chocking of filter pipe lines, fuel pump lines thereby hindering the combustion process (Jain & Sharma, 2012). Wan Nik et al. (2005) improved biodiesel's thermal stability by addition of additives (Irgalube F10). This additive is used as anti-oxidants. Jain et al. (Jain & Sharma, 2012) also used anti-oxidants to improve onset temperature of thermal decomposition of biodiesel. Higher amount of additive usage improved their biodiesel's onset temperature more.

2.5 Lubricating properties

Lubrication property of biodiesel fuel represents its friction and wear from sliding components. Biodiesel has better lubrication properties and high cetane rating compared to diesel fuel (Jayed et al., 2011). Life cycle, material strength, reliability and maintenance cost of fuel injection equipment depends on the lubrication performance of the fuel. Therefore, using biodiesel extends the life of diesel engine due to its better lubricating characteristics compared to petroleum diesel fuel (Atadashi et al., 2011). When two surfaces in contact move relative to each other, friction between the surfaces generates thermal and kinetic energy. At the beginning, from rest to motion first the friction occurs is due to static friction after that during full motion the friction is due to dynamic or kinetic

friction. The time in between is considered as the transition of unsteady state to steady state level (Fazal et al., 2013). Static friction is generally higher than dynamic friction in value. Presence of ester groups in pure biodiesel and increased amount of ester molecules which can enhance the bonding of molecules. In addition, presence of higher amount of oxygen in biodiesel helps to reduce the wear and friction between the contact surfaces (Habibullah et al., 2015). Length of fatty acid chain plays an important role in forming a film between the metal contact surfaces. This film works as a protective film and reduces thermal energy in sliding contact improving its lubricity (Havet et al., 2001; Hu et al., 2005; Knothe & Steidley, 2005).

2.6 Theory of tribology

Tribology is a science of relative motion between interacting surfaces. It is a branch of materials sciences, mechanical engineering and applied mechanics. Tribology includes the boundary-layer contacts either between the two solids surfaces or between the solids and liquids or gases. Tribology covers the field of friction and wear, including lubrication. Primary objective of tribology is to optimize the friction and wear characteristics for an application. In addition, assures sufficient reliability and high efficiency (Kovaříková et al., 2009).

2.6.1 Friction

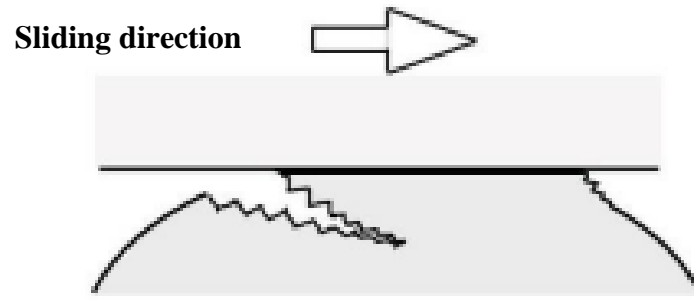
Friction is a force occurs during relative motion of solid metal surfaces, fluid layers, and material elements gliding against each other. When surfaces in contact move relative to each other, the friction between the two surfaces converts kinetic energy into thermal energy. A good example of this property is rubbing pieces of wood together to start a fire. Another example is temperature rise when a viscous fluid is stirred. However, not all friction is desirable. Friction can cause wear, which may lead to performance degradation and/or damage to moving components.

2.6.2 Coefficient of friction (CoF)

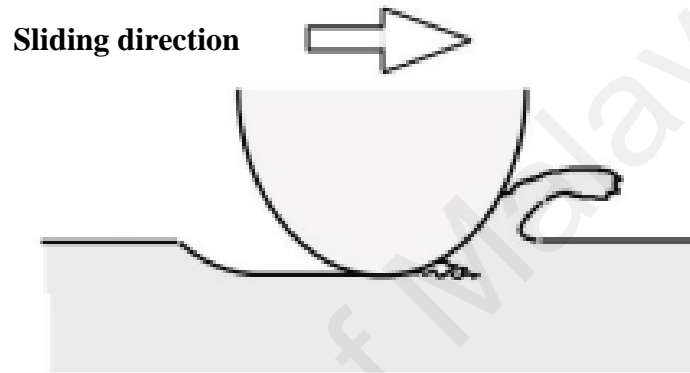
CoF is a dimensionless scalar value which describes the ratio of the force of friction between two bodies and the force pressing them together and often symbolized by the Greek letter μ . The value of CoF typically depends on materials used. For example, ice on steel has a low coefficient of friction, while rubber on pavement has a high coefficient of friction. The higher the CoF, the more two moving surfaces tends to stick together.

2.6.3 Wear

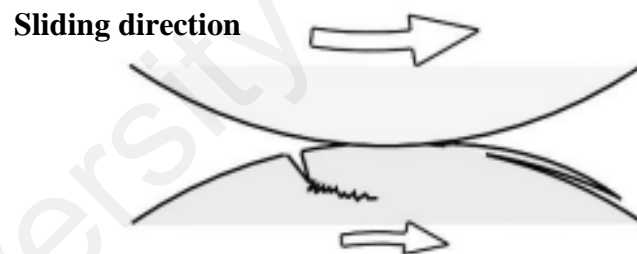
In materials science, wear is erosion or displacement of material from its "derivative" and original position on a solid surface achieved by the action of another surface. Wear is related to interactions between surfaces and more specifically the removal and deformation of material on a surface because of mechanical action of the opposite surface (Liu et al., 1996). Wear can also be defined as a process where interaction between two surfaces or bounding faces of solids within the working environment results in dimensional loss of one solid, with or without any actual decoupling and loss of material. Aspects of the working environment which affect wear include loads and features such as unidirectional sliding, reciprocating, rolling, and impact loads, speed, temperature, but also different types of counter-bodies such as solid, liquid or gas and type of contact ranging between single phase or multiphase, in which the last multiphase may combine liquid with solid particles and gas bubbles (Archard & Hirst, 1956; Dong et al., 2001). **Figure 2.5** shows the different types of wear mechanism. Some commonly referred to wear mechanisms are discussed below:



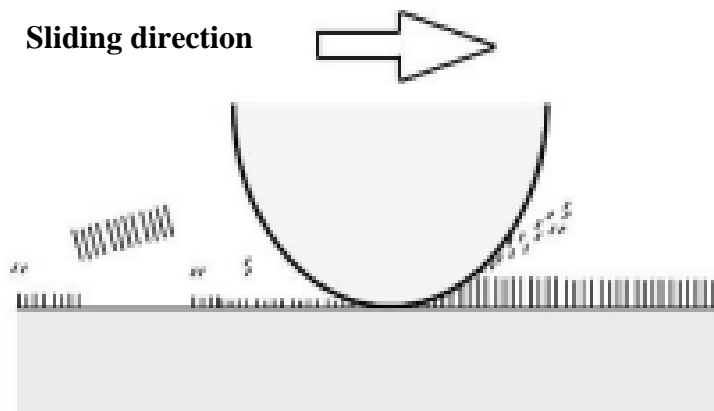
(a)



(b)



(c)



(d)

Figure 2.5: Schematic diagram of different types of wear (Bhushan, 2000)

2.6.3.1 Adhesive wear

Adhesive wear can be found between surfaces during frictional contact and normally refers to unwanted attachment and displacement of wear debris and material compounds from one surface to another. The adhesive wear is caused by the relative motion, plastic deformation and direct contact between the rubbing surfaces, which are created more unwanted wear debris on the surface and transferred material from one surface to another (Wu et al., 2006).

2.6.3.2 Abrasive wear

When the contact interface between the harder and softer surfaces has interlocking of a curved or inclined contact, ploughing take place in the sliding portion. Because of ploughing, a certain volume of surface material is removed and an abrasive groove is formed on the softer surface. This type of wear is called abrasive wear. Abrasive wear can occur when hard material surfaces is rubbing against soften material surfaces. Per ASTM international definition, this is the loss of materials due to hard particles are moved and forced against soften surface (Stachowiak, 2006).

2.6.3.3 Corrosive wear

When sliding take place, particularly in corrosive gases or liquids, the chemical or electrochemical interactions produces some reaction products on the contact surface. If these reaction products are strongly adhering to the surface and their behavior look like the bulk material, the mechanism of wear nearly similar as that of the bulk material. On other hand, the behavior of some reaction products is very different from the bulk material. Hence, the wear mechanism is quite different from that of bulk material, and it is dominated by the reaction products, which are formed by the interactions of solid materials with the corrosive environment. This type of tribo-chemical wear is being accelerated by the corrosive agent is called corrosive wear. In corrosive wear, a reaction

layer is formed on the surface by the tribo-chemical reaction. At the same time, such layer is removed by friction (Kato & Adachi, 2001).

2.6.3.4 Fatigue wear

The phenomenon occurred when a process metal removed by cracking and pitting when the surface of the material is weakened due to cyclic elastic loading or stress during rolling and sliding. Fatigue wear particles will be generated when worn-off surface separately by the cyclic crack growth of micro-cracks on the surface (Atwood et al., 2011).

To summarize the literature review, it can be concluded that the inclusion of emulsion is not always improve properties. It increases viscosity which is not desirable in engine to be used as fuel. However, it does not have humid effect on the chamber as it surrounded with the surfactant. Water in biodiesel emulsion of water in diesel emulsion both have their advantages and disadvantages which we can get from the literature. These are as follows:

Table 2.2: Advantages and disadvantages of diesel and biodiesel emulsion

Advantage	Disadvantage
<ul style="list-style-type: none"> • Lower NO_x emission • Increase homogenous auto-ignition • Reduced knocking • Reduced fuel consumption (in few cases) 	<ul style="list-style-type: none"> • Surfactant is • Higher viscosity may lower the performance • Low calorific value

It is more clear that very few studies been made in the field of oxidation and thermal stability. Also the lubrication properties of biodiesel emulsion is a rare research which need more investigation.

CHAPTER 3: METHODOLOGY

3.1 Preparation of biodiesel emulsion and comparison of emulsifiers

For experimental purposes safety was considered as primary concern. For this wearing lab coat, using hand gloves and cleaning instantly if any chemical drops and also cleaned all the equipment properly just after the use were mandatory.

Palm oil methyl ester is used as base oil and is collected from SIME DARBY BIODIESEL SDN. BHD. in Malaysia. The properties of base oil are provided in **Table 3.1** provided by the supplier.

Table 3.1: Fuel property of Palm oil methyl ester (B-100)

Test	unit	methods	Results
Easter content	% (m/m)	EN14103	98.0
Monoglyceride content	% (m/m)	EN14105	0.4
Diglyceride content	% (m/m)	EN14105	0.1
Triglyceride content	% (m/m)	EN14105	0.04
Total glycerine	% (m/m)	EN14105	0.122
Cetane number	-	ASTM D6890	69.7
Density	Kg/m ³	ASTM D4052	875.2
Kinematic Viscosity	mm ² /s	EN ISO 3140	4.5
Oxidation Stability	hours	EN15751	19.6

Palm biodiesel was used for preparation of biodiesel emulsion. To prepare emulsion surfactant (S) and co-surfactant (C) are used in S:C = 2:1 ratio. Amount of co-surfactant is kept half of the base surfactant. Because, presence of high amount of alcohol as co-surfactant in emulsified fuel will not be favorable as alcohol reduces Cetane number, flash point and affects other fuel properties (Kwanchareon et al., 2007; Shahir et al., 2014). To prepare thermodynamically stable emulsion the following steps were followed and in figure 3.1 the illustration of steps are given.

1. In 80 ml of base oil 3 ml water is mixed separately.
2. Surfactant is then added to three mixtures separately and mixed by shaking the container with hand.

3. Step 2 continues until it forms one phase clear solution
4. After formation of three types of thermodynamically stable emulsions with each surfactant, viscosity is measured of each sample

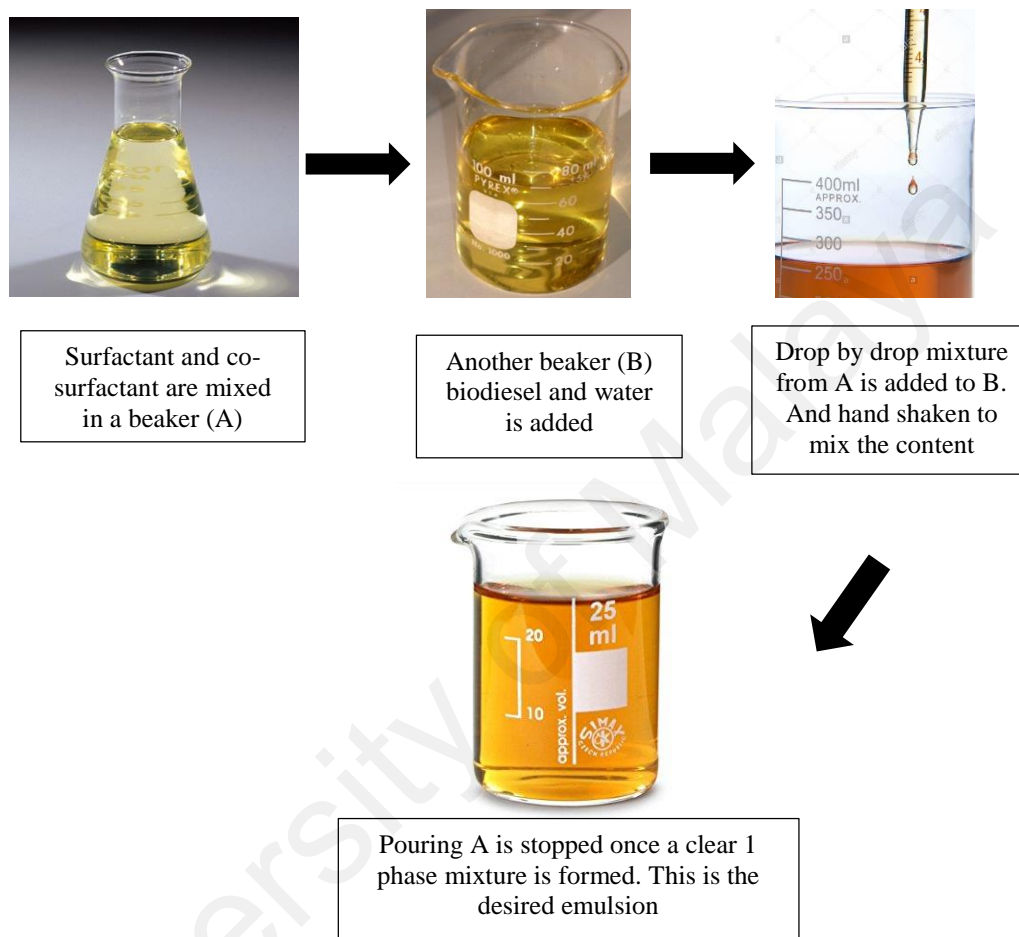


Figure 3.1: Emulsion preparation

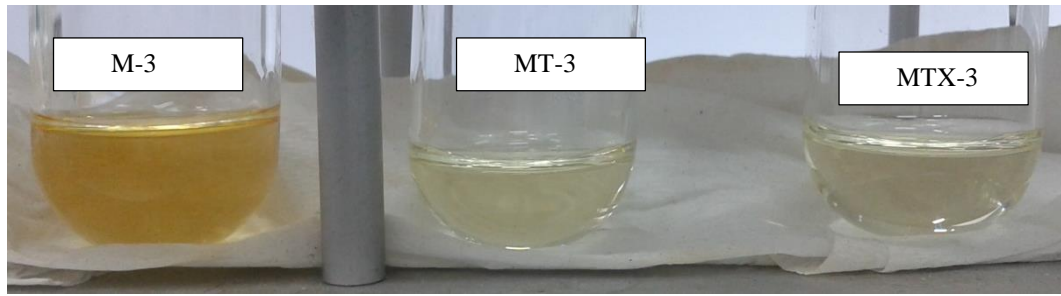
Table 3.2 gives the final composition in percentage for each prepared sample. M-3 emulsion is prepared with Span80 surfactant, MT-3 emulsion is prepared with Tween80 surfactant and MTX-3 emulsion is prepared with TritonX-100 surfactant. Ethanol is used as co-surfactant for all samples. Prepared emulsions were water in oil (W/O). To check emulsion type, a small quantity of each emulsion is taken as shown in **Figure 3.2(a)**. Then few drops of oil (B-100) is added to each sample and in the next round few drops of water is added to each sample. After addition of both oil and water separately the change in solution was observed. It is shown in **Figure 3.2(b)** that after addition of oil no change in

emulsion is visible. However, addition of water destabilized the emulsion as shown in the **Figure 3.2(c)**. Therefore, oil is in continuous phase in the prepared samples; i.e., the samples are W/O emulsion.

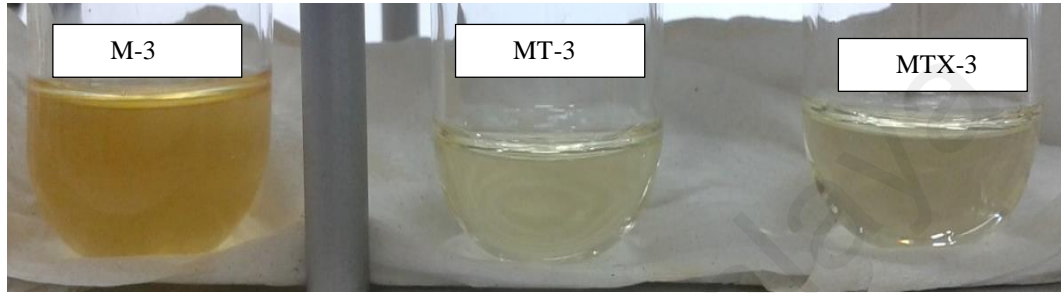
Table 3.2: Properties of emulsion prepared from three surfactants

Sample	Composition			Number of Layer	Time to stabilize	Density g/cm ³	Viscosity mm ² /s
	B-100	Water	S+C				
M-3	80 mL	3 mL	111 mL	1	5 min	0.8984	9.8792
	41.3v/v%	1.5 v/v%	57.2 v/v%				
MT-3	80 mL	3 mL	34 mL	1	Instant	0.9025	16.572
	68.4 v/v %	2.6 v/v %	29 v/v %				
MTX-3	80 mL	3 mL	22 mL	1	Instant	0.8932	9.9827
	76 v/v %	3 v/v %	21 v/v%				

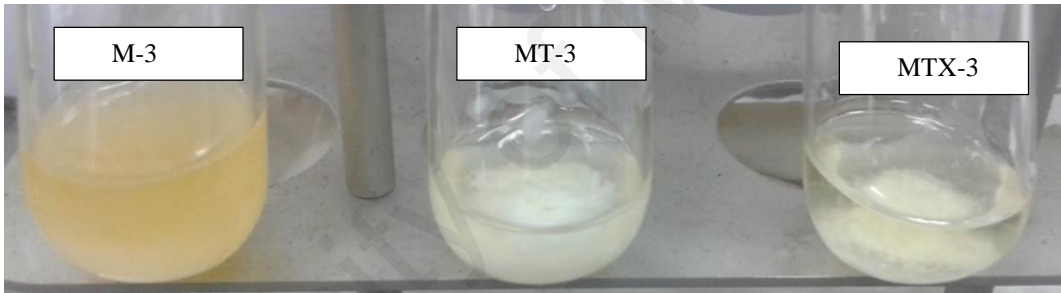
From **Table 3.2**, it can be observed that amount of span 80 is much higher than tween 80 and tritonX-100. MTX-3 required least amount of surfactant to prepare emulsion with 3ml water. About 57% surfactant including ethanol is required to prepare 1 phase solution. For tween80 about 29% surfactant including ethanol is required to prepare emulsion. However, about 21% TritonX-100 and ethanol is required for emulsification. Therefore, preparation of emulsion with TritonX-100 requires minimum amount of surfactant compared to Tween 80 and Span 80. Moreover, M-3 and MTX-3 has lower viscosity and density compared to MT-3. Therefore, MTX-3 requires least amount of surfactant which is cost effective and has better fuel property. Therefore, for further investigation TritonX-100 surfactant is used to prepare samples. Samples prepared are with 1 ml water (1% water), 2 ml water (2% water) and 3 ml (3% water) water in 80 ml B-100 separately. Produced samples are named MTX-1 (1% addition of water), MTX-2 (2% addition of water) and MTX-3 (3% addition of water). Amount of surfactant used also varied for each sample.



(a) Initial solution



(b) After addition of B-100



(c) After addition of water

Figure 3.2: Emulsion type identification test

3.2 Zetasizer

Zetasizer widely used equipment for the measurement of size, electrophoretic mobility of proteins, zeta potential of colloids and nanoparticles. For this study zetasizer is used to measure the size of water droplets and its distribution in biodiesel emulsion. To measure the droplet size sample needs to be filled up to 10 to 15mm of the cell. This cell comes with the zetasizer which is then inserted in the equipment. **Figure 3.3** shows the Zetasizer connected with a computer which is used for this study.

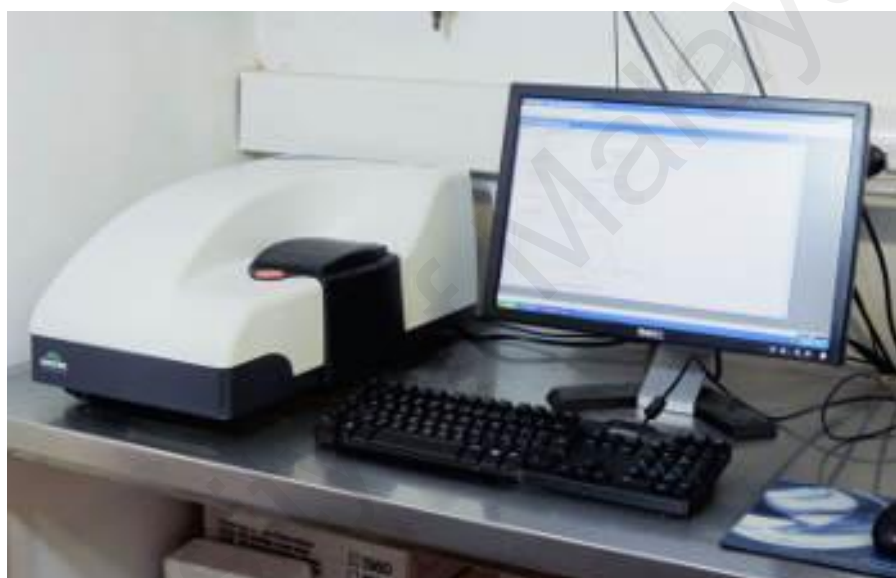


Figure 3.3: Zetasizer equipment set up for droplet size measurement

3.3 Optical microscope

The optical microscope, often stated to as the "light microscope", is a type of microscope which uses visible light and a system of lenses to magnify images of small samples. Optical microscopes are the oldest and simplest of the microscopes ("Optical microscope," 2008). To view the water droplet in emulsion OPTIKA B – 600 optical microscopes was used. On the glass plate a small drop of sample was placed. Then adjusting the lenses the pictures of the droplet distribution was captured. **Figure 3.4** shows the optical microscope used for this study.



Figure 3.4: Optical microscope used to visualize water droplet in emulsion

3.4 Fuel properties measuring procedure and equipment

Viscosity, calorific value, density, oxidation stability, flash point, pour point, cloud point- these are the properties that determines the quality of the produced biodiesel. The important physical and chemical properties of the produced biodiesels were tested according to ASTM D6751 standard. **Table 3.3** provides the detailed manufacturing information of the equipment used to study biodiesel properties.

Table 3.3: Information of the equipment used for fuel property measurement

Property	Equipment	Manufacturer	Test method	Accuracy
Kinematic viscosity	SVM 3000	(Anton Paar, UK)	ASTM D445	±0.1%
Density	SVM 3000	(Anton Paar, UK)	ASTM D1298	±0.1 kg/m ³
Oxidation stability	873 Rancimat	(Metrohm, Switzerland)	EN ISO 14112	±0.01 h
Calorific value	C2000 basic calorimeter	(IKA, UK)	ASTM D240	±0.001 MJ/kg

3.4.1 Density and viscosity measurement

Density is the ratio of mass to volume and viscosity represents flow resistance of a fluid. In order to measure density, Anton Paar automatic viscometer (SVM 3000) was used in this study (**Figure 3.5**). It can be used to measure the dynamic viscosity (mPa.s) and density (g/cm³) of the fuel according to ASTM D7042. From this result, the viscometer automatically calculates the kinematic viscosity and delivers measurement results which are equivalent to ISO 3104 or ASTM D445. As density result is needed to calculate the kinematic viscosity from the dynamic viscosity a density measuring cell in SVM 3000 has been given. Both cells are filled in one cycle and the measurements are carried simultaneously. At first a self-test will be done and the initializing procedure will be performed by SVM, and then it will be ready for measurement. Until the results of the first repetition are within the limits for the viscosity and density, the state will not change to 'result valid' and one more refill will be required in order to continue measurement.



Figure 3.5: Viscometer

Rotational viscosity measurement is based on a torque and speed measurement. A rotating magnet in the SVM 3000 produces an eddy current field with an exact speed-dependent brake torque. Some technical data is provided in **Table 3.4**. The eddy current torque is measured with extremely high resolution. Combined with the integrated thermoelectric thermostating, this ensures unparalleled precision. The torque resolution is an unmatched 50 pico-Nm. That's why it only requires a very compact measuring cell. The very small measuring cell contains a tube which rotates at a constant speed. This tube is filled with the sample. Floating in the sample is a measuring rotor with a built-in magnet. The low density of the rotor allows it to be centered by the centrifugal force. The freely swimming rotor requires no bearing - and where there is no bearing, there is no friction. This also makes the instrument insensitive to vibration. The small sample volume allows extremely quick temperature changes (Peltier) and very short equilibrium times. Shortly after the start of the measurement the rotor reaches a stable speed. This is determined by the equilibrium between the effect of the eddy current brake and the shear forces at work in the sample. The dynamic viscosity is calculated from the rotor speed.

Table 3.4: Technical data for Anton paar (SVM 3000) viscometer

Parameter	Values
Dynamic viscosity (mPa.s)	0.2-20000
Density (g/cm ³)	0.65-3
Temperature (°C)	15-105
Repeat deviation of viscosity	0.1%
Repeat deviation of density (g/cm ³)	0.0001
Space requirements L×W×H(mm)	440×315×220

3.4.2 Calorific value

The heating value of all the fuel samples used in this research work was determined using IKA C 2000 calorimeter. IKA C 2000 calorimeter system shown in **Figure 3.6** can be used to determine the gross calorific value of solid and liquid materials in accordance to DIN 51900, BS 1016 T5, ISO 1928, ASTM 5468 and ASTM D240. Some technical data of the calorimeter can be found from **Table 3.5**.



Figure 3.6: Calorimeter

The combustion calorimeter measures the heat that rises from burning of fuel sample. The sample is weighed into a digestion vessel and filled with oxygen. The burning process is started by means of an ignition spark. The experiment ends when the sample is fully burned. By measuring the temperature increase, the heating value of the sample can be calculated. In more detail, it can be said that combustion process in IKA C 2000 calorimeter takes place under defined conditions. To fulfill this condition, the decomposition vessel is coated with a weighed-out quantity of fuel sample, the fuel sample is ignited, and the increase in temperature of the calorimeter system is measured.

The specific gross calorific value of the sample is calculated from the following parameters:

- The weight of the fuel sample
- The heat capacity value of the calorimeter system.
- The increase in temperature of the water within the inner vessel of the measuring cell.

Table 3.5: Technical data of calorimeter

Parameters	Value
Duty cycle	Continuous operation
Ambient Temperature	20°C ... 25°C (constant)
Ambient relative humidity	80%
Usage above sea level	2000 meters above sea level
Measurement range	40,000 J
Measuring mode	Isoperibolic 25°C
	Dynamic 30°C
	Isoperibolic 30°C
	Dynamic 25°C
Isoperibolic measuring time	About 22 min
Dynamic measuring time	About 10 min
Oxygen operating pressure	30 bar
Oxygen test pressure	40 bar
Cooling medium	Water via line
Dimensions	440 x 450 x 500 (W x D x H)
Weight	30 kg
Flow quantity	Min. 60 liters/hour
	Max. 70 liters/hour

3.4.3 Oxidation stability

Biodiesel derived from vegetable oil has double bond molecules in free fatty acid. Presence of double bond make biodiesel vulnerable to oxidation when subjected to high temperature and contact to the oxygen of the air. Therefore, it is important to measure the oxidation stability of biodiesel and biodiesel emulsion. In this study oxidation stability was measured by induction period. Oxidation stability of samples was evaluated with commercial appliance Rancimat 743 as shown in **Figure 3.7** applying accelerated oxidation test (Rancimat test) specified in EN 14112. The end of the induction period (IP) was determined by the formation of volatile acids measured by a sudden increase of conductivity during a forced oxidation of ester sample at 110°C with airflow of 10 L/h passing through the sample. Some technical data is given in



Figure 3.7: Biodiesel Rancimat

Table 3.6: Technical data of Rancimat

Parameter	Values
Sample size	Liquid samples: 3.0 ± 0.1 g
Measuring solution	60 mL
Temperature ($^{\circ}\text{C}$)	80-160
Gas Flow	10 L/hr
Evaluation	Induction time
Evaluation sensitivity	1.0

3.5 FT-IR analysis

Characterization of diesel and biodiesel were performed through FT-IR using Perkin–Elmer biodiesel FAME analyzer which is connected to an MIR TGS detector (**Figure 3.8**). The spectrum range was $4000\text{--}400\text{ cm}^{-1}$, and resolution and scans were 4 cm^{-1} and 16, respectively. The spectrum was processed by e-spectrum software.



Figure 3.8: FT-IR spectrometer

3.6 Proton NMR analysis

NMR analysis of biodiesels was conducted by using a Bruker Ascend™ 600 MHz NMR spectrometer (**Figure 3.9**) with a 5 mm PABBO BB probe for ^1H spectroscopy observation at 299 K. The spectra for ^1H is obtained at 600 MHz for 15 min and 5 h duration for ^1H , respectively. Deuterated chloroform (CDCl_3) was used as solvent. Few drops of sample is given in the test tube and rest is solvent up to the mark given in the tube. ^1H spectra were obtained with 30° pulse duration, a recycle delay of 1.0 s and 16 scans.



Figure 3.9: NMR spectrometer

3.7 TGA and DSC analysis

The TGA analysis test of biodiesels and diesel was performed by using TGA Q500 V20.13 Build 39 thermal analyzer (**Figure 3.10**). The test was performed at a constant heating rate of 50 °C/min under nitrogen atmosphere at a flow rate of 40 ml/min. About 10-20 mg of samples were used in a 40 µL platinum pan at temperature interval from 4.0 °C- 950 °C. The DSC analysis test of biodiesels and diesel was performed in an instrument named DSC Q200 V24.11 Build 124 (**Figure 3.11**). DSC analytical module in standard cell under inert (nitrogen) atmosphere with gas flow rate of 50 ml/min and at a 10 °C/min heating rate to 130 °C to heat the samples. DSC cell was loaded with one sample and one reference pans. About 10 mg of sample was put in sealed in an aluminum pan and one identical empty pan was set as a reference to perform the test. For heating scans, samples were cooled rapidly and held isothermally for 2 min at -60 °C and then heated to 130 °C and then the samples were held isothermally for 2 min at 130 °C, then cooled to -80 °C for cooling scans.

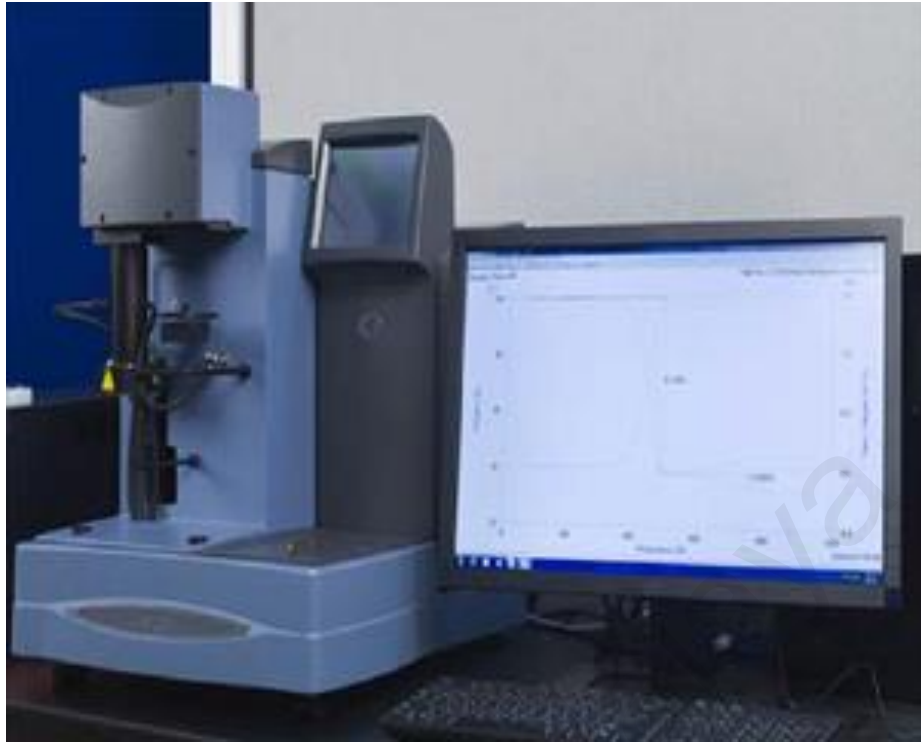


Figure 3.10: Thermo-gravimetric analyser



Figure 3.11: DSC analyser

3.8 Experimental setup and testing procedure of 4-ball tribo tester

A 4-ball tester (TR-30H) was used to observe the friction and wear characteristics of biodiesel emulsion. **Figure 3.12**, shows the schematic diagram of four ball tribo tester. To perform the test MTX-2 has been selected as test sample as it has better physicochemical property, oxidation stability and thermal stability compared to MTX-1 and MTX-3. With MTX-2, two biodiesel-diesel blends (BTX-5 and BTX-10) were prepared for this experiment. Composition of BTX-5 and BTX-10 is provided in **Table 3.7**. BTX-5 was prepared with and BTX-10 was prepared with 10% MTX-2 and 90% diesel.

Table 3.7: Composition of biodiesel-diesel blend

Name	Composition
BTX-5	5% MTX-2 + 95% diesel
BTX-10	10% MTX-2 + 90% diesel

Friction and wear test was performed using B-100, MTX-2, BTX-5, BTX-10 and neat diesel. Here, three balls remain stationary and one ball at the top rotates around the three balls. All the balls were washed with toluene and wiped dry with tissue. Three balls were kept fixed in a steel cup. Test oil of 10 ml was poured in the cup so that the balls were covered with test oil with 3mm depth covering the surface of the balls. The fourth ball adjusted with collet. Winducom software was used to store the tested results in a computer. This test was performed according to ASTM 4172 standard with load 40 kg and temperature 75 °C. Experimental test conducted with 1200 rpm for 3600 s. **Table 3.8** shows the operating condition of four ball tester and ball specification. Co-efficient of friction (CoF) was calculated by using the equation 1.

$$Co - efficient\ of\ friction(CoF), \mu = \frac{Frictional\ torque\ (kg-mm) \times \sqrt{6}}{3 \times applied\ load\ (kg) \times distance(mm)} \quad (1)$$

Distance measured from the center of the lower ball contact surface to the rotation axis was 3.67 mm. After completion of test, the wear scar diameter (WSD) of the stationary balls were measured by an optical microscope modeled C2000, IKA, UK. Further tests were performed using SEM/EDX analysis. SEM, scanning electron microscope is a type of electronic microscope that produces images by scanning it through focused beam of electrons. Energy-dispersive X-ray spectroscopy (EDX) is an analytical technical technique used for the elemental analysis and chemical characterization of the oil sample.

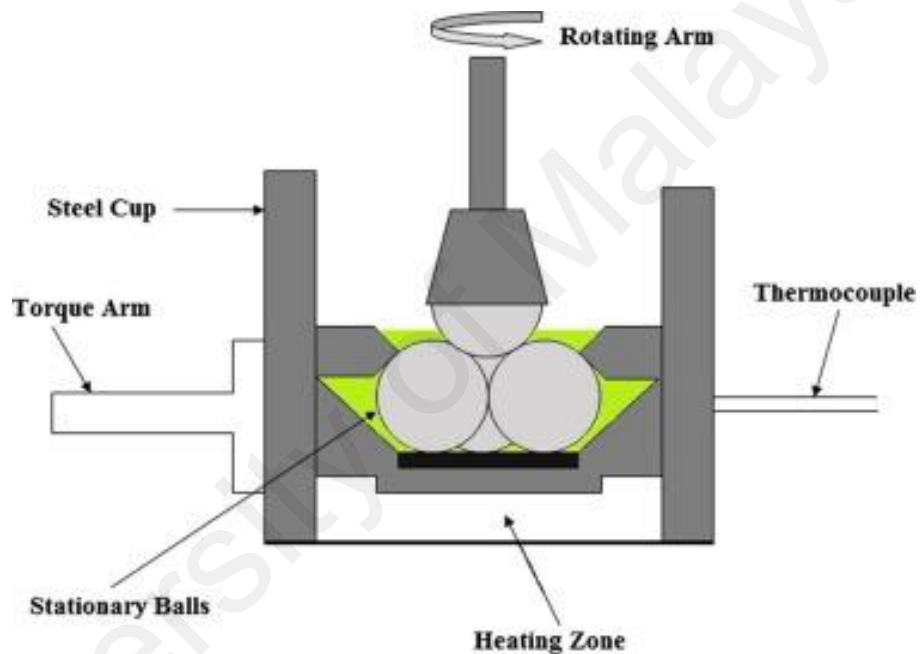


Figure 3.12: Schematic Diagram of 4 ball tribo tester

Table 3.8: Experimental operating conditions for four ball machine

Parameters	Condition
Machine operating conditions	
Load	40 kg
Speed	1200 rpm
Temperature	75 °C
Test duration	3600 s
Standard	ASTM D4172
Testing Ball specification	
Materials	Chrome alloy steel (SKF)
Size	∅ (12.7 mm)
Hardness	62 HRC
Composition	10.3% C, 0.08% S, 1.43% Cr, 0.11% P 0.42% Mn, 0.05% Ni, 0.47% Si, 2.12% Zn and rest 85.02% Fe
Surface roughness	0.1 µm (C.L.A)

CHAPTER 4: RESULTS AND DISCUSSION

4.1 Introduction

In this chapter, the results of all analysis done throughout the research are presented and discussed. At first, preparation of biodiesel emulsion with three surfactants are discussed and compared. After that, physicochemical properties, bond characteristics and thermal properties of biodiesel emulsion were fully covered and presented. Finally, lubrication properties of emulsified biodiesel are analyzed. All the findings are accumulated in discussion section for comparison and assessment of biodiesel emulsion compared to neat biodiesel and diesel fuel.

4.2 Physicochemical properties of emulsified palm oil methyl ester

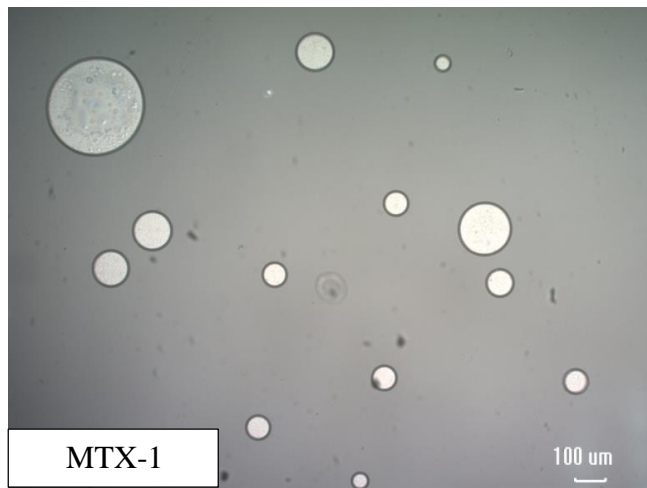
From **Table 4.1**, it is observed that the fuel property of emulsified fuel is changed due to addition of water. Density is increased and as well as viscosity with the addition of water. Calorific value is reduced due to presence of water. This can be explained as in emulsified fuels the percentage of B-100 is reduced with increase in water content. Therefore, calorific value is reduced as less percentage of B-100 is present in emulsified biodiesel compared to neat biodiesel. Ash content is reduced with the increase of water addition. The oxidation stability is increased with the increasing water concentration. MTX-1 and B-100 has same oxidation stability time. But oxidation stability of MTX-2 is 102% higher than diesel and 27% higher than biodiesel. MTX-3 has 110% and 32% higher oxidation stability time from diesel and biodiesel respectively. The percentage changes are calculated by simple arithmetic rules ($\%change = \left| \frac{Diesel\ or\ Biodiesel-sample}{Diesel\ or\ Biodiesel} \right| \times 100\%$). This is a desirable improvement of biodiesel as it is vulnerable to oxidation. As, in general, biodiesel has relatively poorer oxidation stability compared to that of diesel fuel (Rizwanul Fattah, Masjuki, et al., 2014; Xin et al., 2008).

Table 4.1: Fuel property of emulsified biodiesel

Name	Composition			Density, (kg/m ³)	Viscosity, (mm ² /s)	Calorific Value, (J/g)	Ash content (%)	Oxidation stability, (hr)
	B-100 mL	S+C mL	Water mL					
Test Method	-	-	-	ASTM D1298	ASTM D445	ASTM D240	-	EN ISO 14112
Diesel	-	-	-	839.1	3.72	45670	0.54	12.36
B-100	100	-	-	875.2	4.5	39963	0.35	19.6
MTX-1	82.5	16.5	1	878.6	6	37781	0.33	19
MTX-2	80	18	2	879.8	7	37499	0.12	25
MTX-3	76	21	3	893.2	10	34037	0.06	26

4.3 Droplet distribution of biodiesel emulsion

Figure 4.1 shows the droplet distribution of three biodiesel emulsion. It can be observed that MTX-1, MTX-2 and MTX-3 have wide range of droplet sizes. Droplet size refer to the diameter of the droplet exist in the emulsion. With increase in water concentration droplet size is reduced. To visualize the exact distribution of droplets Zeta sizer was used. For each sample, tests were done three times which is indicated by three different color of the curves in **Figure 4.2**. In **Figure 4.2** droplet size is in nm scale and d refers to diameter of the droplet. MTX-1 gives one distribution around 1000 nm. MTX-2 gives three distributions on average. This indicates wider variety of droplet size, where the range is from 1000 nm to 10 nm. However, in MTX-3 this droplet size' range is only between 500 nm to 5 nm diameter. MTX-2 has the various sizes of droplets compared to MTX-1 and MTX-3, which indicates better stability of the emulsion. to create a stable emulsion, droplet size plays a significant role. Smaller the size more stable is the emulsion. Moreover, presence of various size of droplets increase stability (Society et al., 2014).



(a)

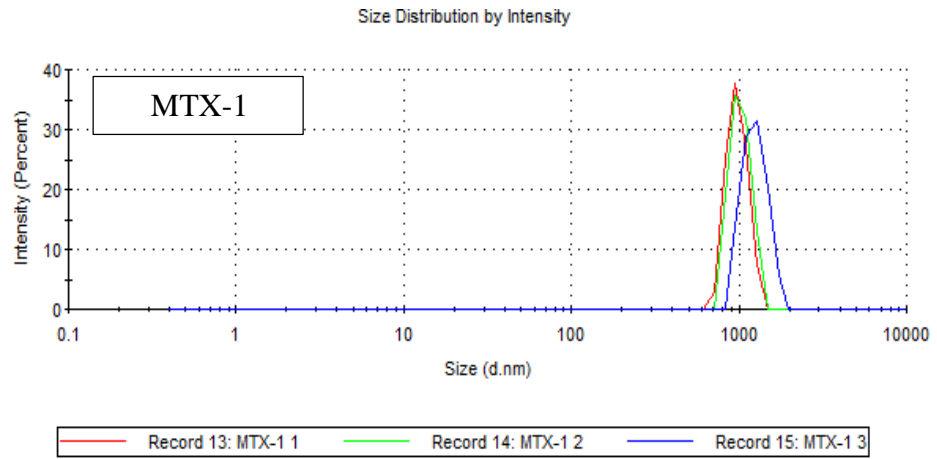


(b)

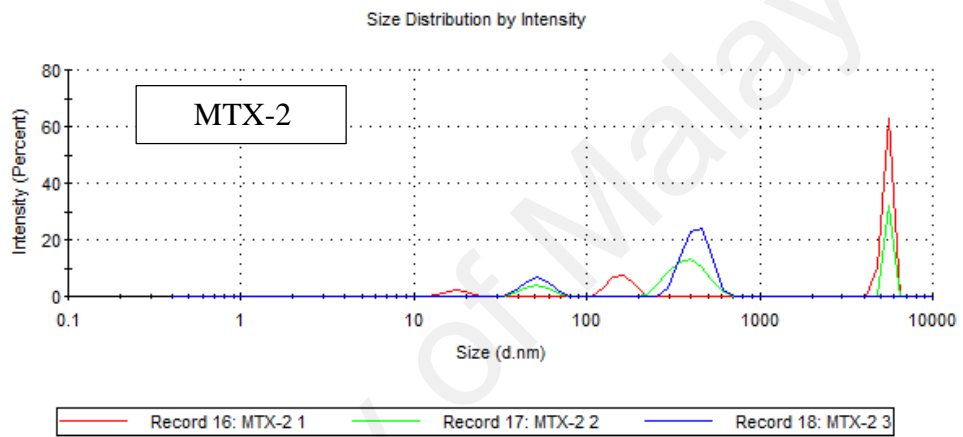


(c)

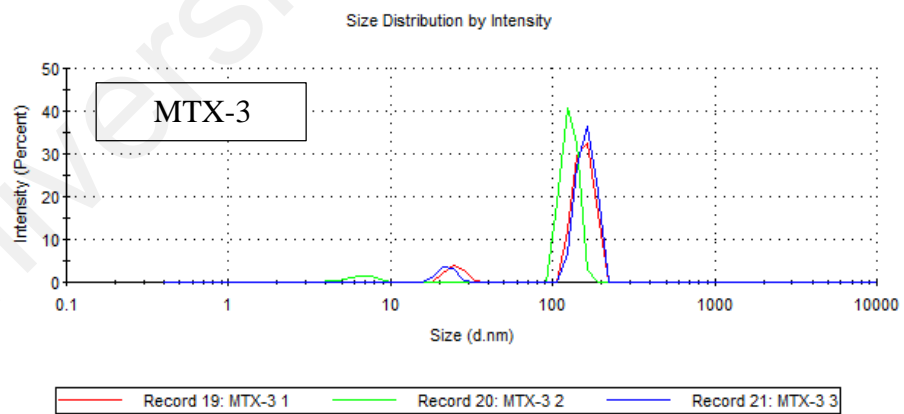
Figure 4.1: This shows the water droplet distribution of (a) MTX-1 (b) MTX-2 (c) MTX-3 through optical microscope.



(a)



(b)

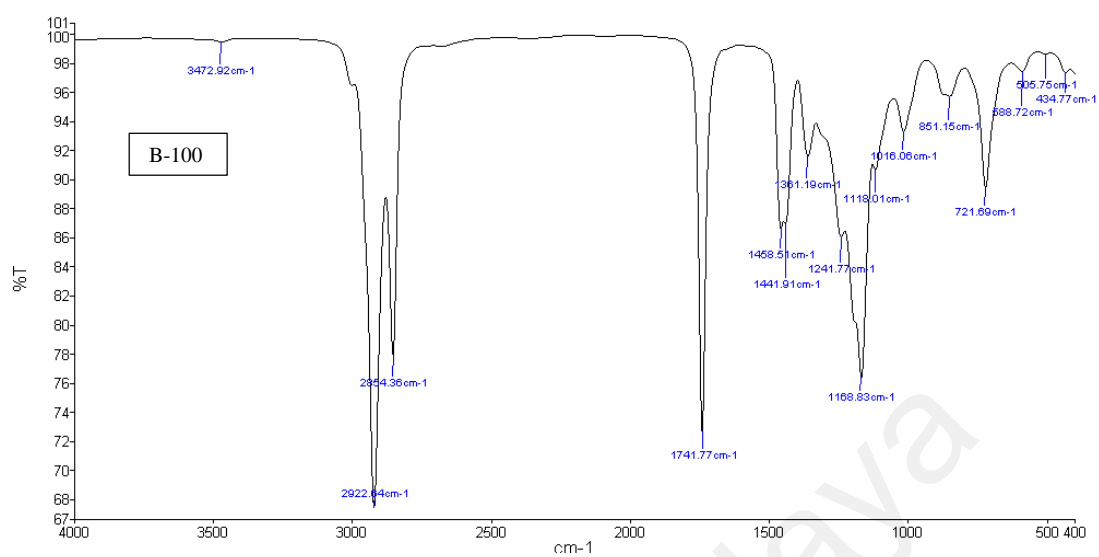


(c)

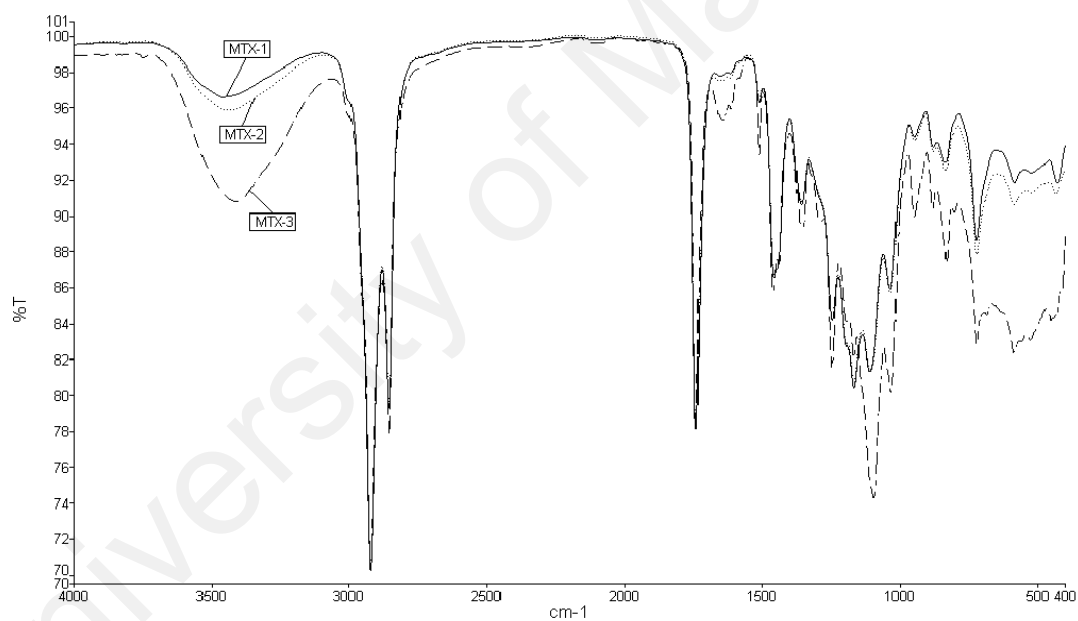
Figure 4.2: This shows the water droplet distribution of (a) MTX-1 (b) MTX-2 (c) MTX-3 with Zeta sizer

4.4 Fourier transform infrared spectroscopy (FTIR) Analysis

Figure 4.3, presents the transmittance curve of neat biodiesel and emulsified biodiesel. **Table 4.2** presents the bond assignment of the signal found from the curve. The presence of water is observed in the $\sim 3473\text{ cm}^{-1}$ broad region. With the increase in water concentration the transmittance is reduced. The presence of terminal methyl group is also seen just after 3000 cm^{-1} and its bending motion at $\sim 1360\text{ cm}^{-1}$. The presence of ester is visible with the three signals in 1742 , 1240 and 1035 cm^{-1} region. Due to presence of benzene ring in surfactant there are three absorptions in 1655 , 1512 , 1458 cm^{-1} region which is absent in B-100's transmission curve. Vinyl group is also seen to present only in the emulsified biodiesel. Due to presence of sulfur and iodine in the biodiesel absorption in the region of 1170 , ~ 500 and $\sim 400\text{ cm}^{-1}$ are observed. It can be seen that within 3000 to 1200 cm^{-1} there is no significant change in the transmission. The results of FTIR show the presence of functional groups in the sample. Unsaturated ester delays ignition, benzene ring forms toxic emission, sulphur and iodine also form toxic gas and particulates



(a)



(b)

Figure 4.3: (a) transmittance (%T) vs wave number (cm^{-1}) curve of B-100 and (b) transmittance (%T) vs wave number (cm^{-1}) curve of MTX-1, MTX-2 and MTX-3.

Table 4.2: FTIR results of B-100, MTX-1, MTX-2, and MTX-3

B-100	MTX-1	MTX-2	MTX-3	Bond Assignment	Remarks
3473	3458 (broad)	3448	3412	O-H Bond	Presence of water
2923 2854	2923, 2855.12	2923 2855	2923 2854	Csp ³ -H	
1742 1242 1036	1740.55 1245 1036	1741 1245 1035	1742 1246, 1293 1032	(C=O) (Csp ² -O) (Csp ³ -O)	Ester
	1655 1512 1458	1660 1513 1458	1665 1512 1461, 1439	(C=C) Aromatic ring C-H Bending motion	
1362	1360	1360	1353	C-H ₃ Bending motion	Terminal methyl group present
1169	1169	1169	1170	SO ₂ sym stretch	
1118	1110.5	1109	1095.5	Alkyle-substituted ether, C-O stretch	
-	945	948	948	CH ₂ out of plane wag (Vinyle compounds)	
851	878 835	878 835	881 830	CH out of plane deformation	
722	721	721	721	(CH ₂)- rocking in methylene chain	
589	585	586	587	O-C-O in ester	
506	523	522	524	Aliphatic iodo compounds, C-I stretch	
435	429	436	463	S-S stretch	

4.4.1 Proton nuclear magnetic resonance ($^1\text{H-NMR}$) analysis:

$^1\text{H-NMR}$ analysis is carried out to observe structural changes in biodiesel due to emulsion and water concentration in emulsion. **Table 4.3**, **Table 4.4**, and **Table 4.5** shows the list of peaks and assignment of bonds of surfactant, biodiesel and emulsified biodiesel. First, B-100 and surfactants peaks assignment are done. After that, the peaks of emulsified biodiesel were first traced using the B-100 and surfactants assignment. The rest peaks are then predicted as water and ethanol and checked if there is any new chemical shift.

From **Table 4.3**, peak at 3.95 is double triplet and is assigned for α proton of oxyethylene near the Aryl group. This is predicted as the associated carbon is bonded to oxygen and has Aryl group as the next neighbor. Chemical shift at 2.9 ppm is considered as the terminal $-\text{OH}$ (Can, 2014). According to this reference the shift should be at 2.3 ppm. As no shift is found at 2.3 ppm, it can be stated that the shift has moved to downfield region due to the presence of oxy ethylene group.

Chemical shifts of B-100 (**Table 4.4**) are assigned molecular positions according to the reference found from previous studies (Can, 2014; Jiang Naoko et al., 2010). **Table 4.5** shows the chemical shifts found in emulsified biodiesel. All the chemical shifts that are found in surfactant and biodiesel should present in biodiesel emulsion- as emulsion process does not involved any chemical reaction. However, few chemical shifts are missing or changed due to forming hydrogen bond with water. Chemical shift at 2.9 ppm present in surfactant has shifted to 3.46 ppm. This may be explained by the hydrophilic tail of the surfactant. This hydrophilic part of surfactant forms bond with water, hence, presence of electronegative molecule shifted the signal to downfield region. Change in chemical shift means change in molecules, which means reaction happened. However, if the chemical shift is within the range then it means the molecule is not changed but due to different environment it is slightly displaced. When there is a reaction and new

molecule comes in then depending on its type it may have contribution during combustion. Multiplet signal at 1.28ppm in emulsified biodiesel is consistent with the B-100 signal found. As shown in **Figure 4.4**, the multiplet signal is further divided in to three types of signals- 1.32, 1.28 and 1.22 ppm. The new signal at 1.22 ppm is due to ethanol used in emulsification. The broad peak found around 1.90 ppm is due to water present in the emulsion. **Error! Reference source not found.**, shows the proton NMR signals found in MTX-1, MTX-2 and MTX-3.

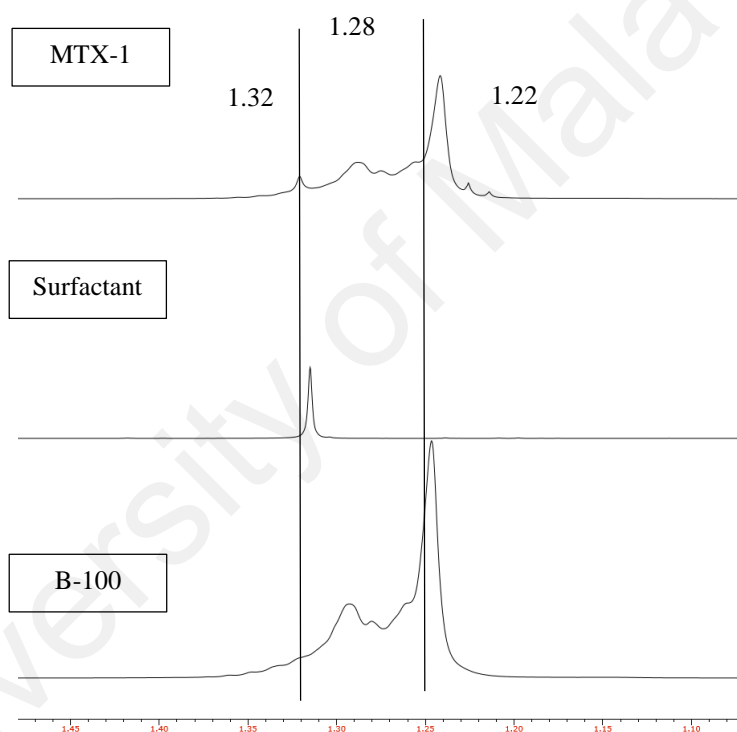


Figure 4.4: ^1H -NMR signals of MTX-1, surfactant and B-100 around chemical shift of 1.3 ppm.

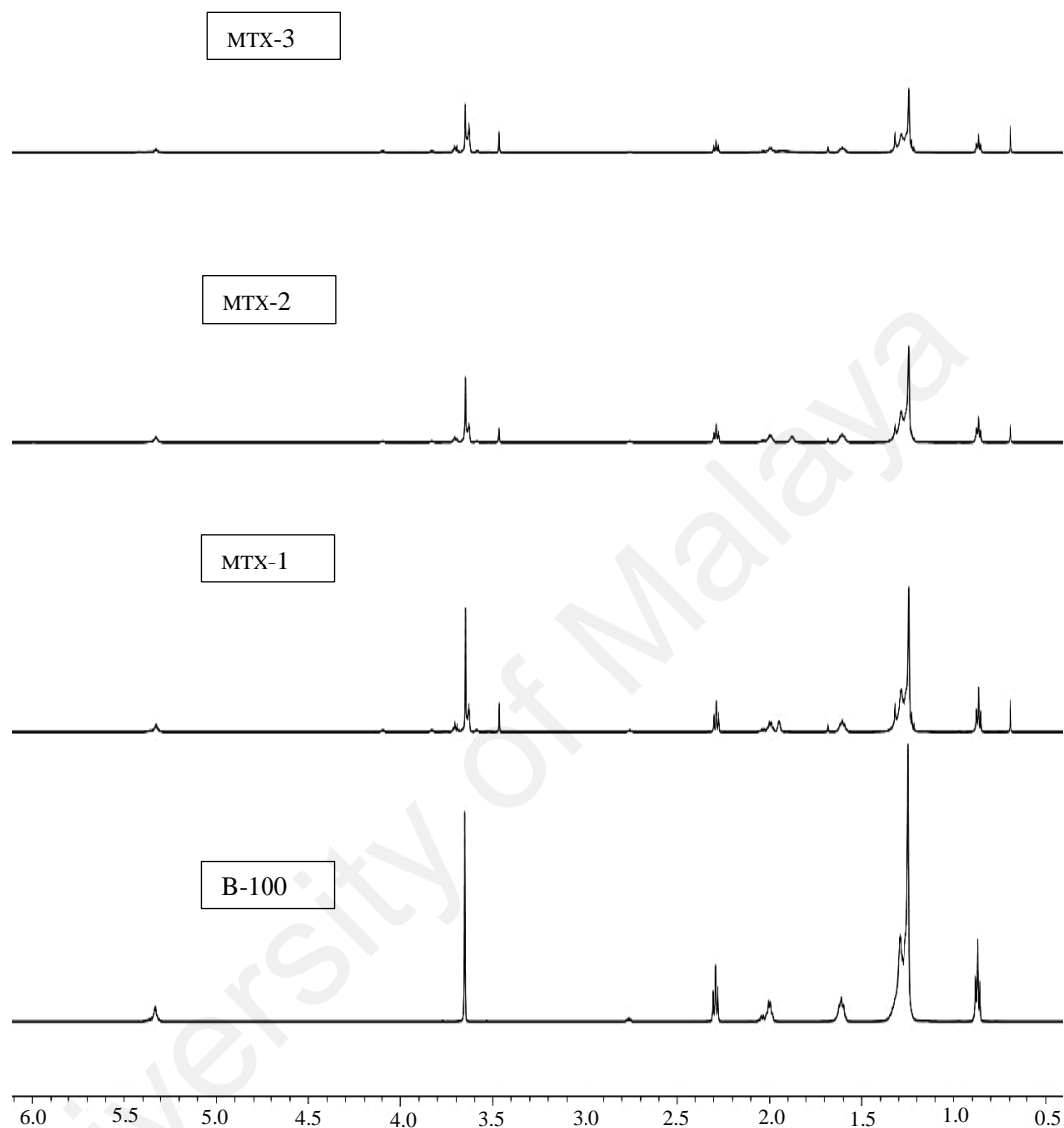


Figure 4.5: Chemical shift of B-100, MTX01, MTX-2 and MTX-3 in ppm.

Table 4.3: ¹H-NMR analysis of Surfactant

Centre ppm (Approx.)	Type of splitting signal	%H	J coupling value	Assignment
6.8	d	4	8.85	Ar-H
3.95	dt	8	158.55,4.96	...-Ar-O-CH ₂ -CH ₂ -.....-O-CH ₂ -CH ₂ -O-H
3.66	m	53	-	Oxy-ethylene protons -(O-CH ₂ -CH ₂)-
2.9	s	3	-	Terminal HO- (Can, 2014)
1.68	s	4	-	(CH ₃) ₃ CH ₂ -
1.31	s	12	-	(CH ₃) ₂ CH ₂ -
0.7	s	17	-	Terminal methyl proton

Table 4.4: ¹H-NMR analysis of B-100

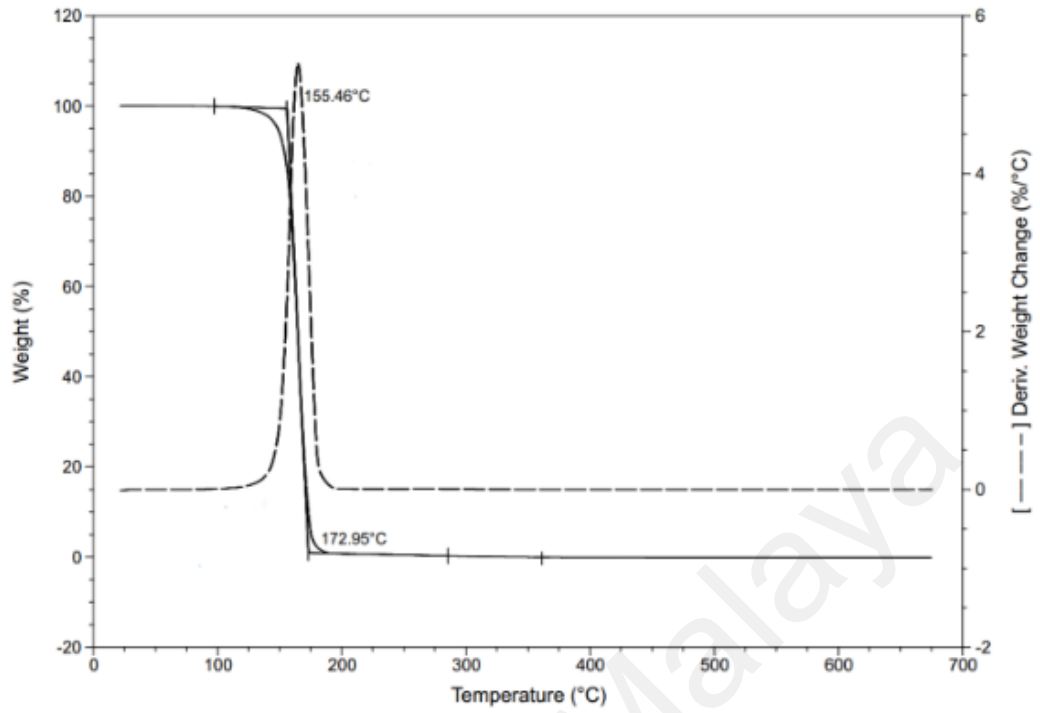
Centre ppm (Approx.)	Type Of splitting signal	%H	J coupling value	Assignment
5.3	m	3	-	Olefinic hydrogens in ester (Madankar et al., 2013)
3.66	s	8	-	Terminal Methoxy proton (Tariq et al., 2011)
2.76	t	1	6.81	di-vinyl methylene protons (due to presence of Methyl Linoleate) (SCIENTIFIC)
2.3	t	6	7.56	α- CH ₂ proton (Tariq et al., 2011)
2	dq	5	22.85, 7.02	Allylic hydrogens (SCIENTIFIC)
1.6	t	6	6.73	β- carbonyl protons (Tariq et al., 2011)
1.28	m	68	-	Methylene protons (Tariq et al., 2011)
0.9	t	8	6.9	Terminal methyl protons (Tariq et al., 2011)

Table 4.5: ¹H-NMR analysis of biodiesel emulsion

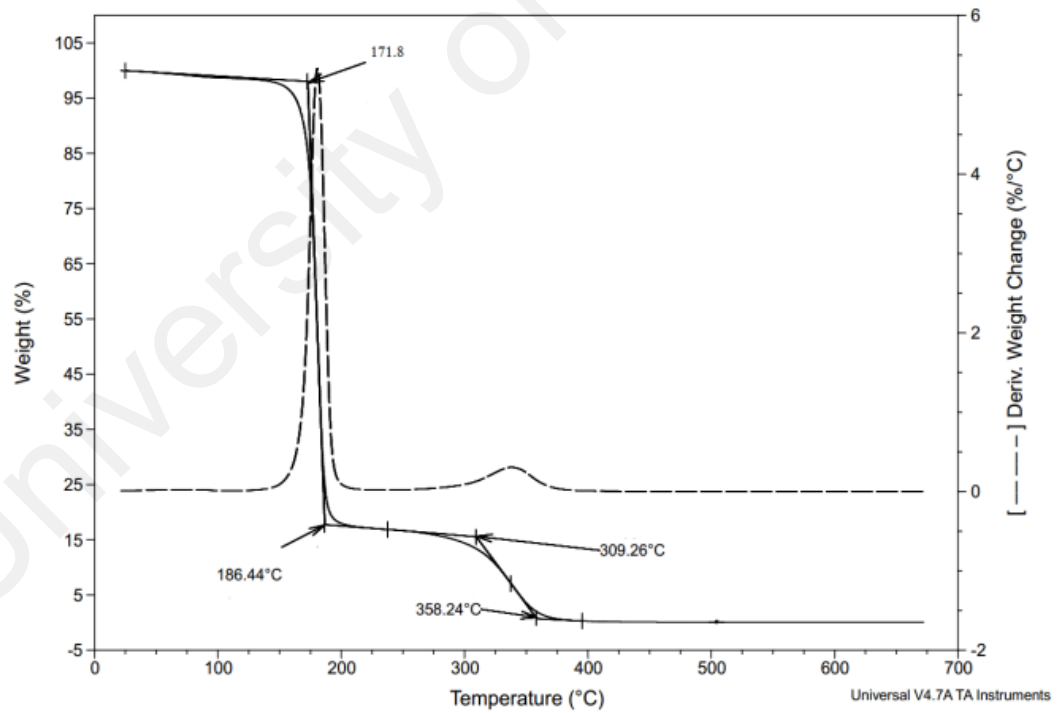
Centre ppm (Approx.)	Type of spitting signal	%H			J coupling value	Assignment
		MTX-1	MTX-2	MTX-3		
6.8	d	0.4	0.4	0.8	8.75	Ar-H
5.3	m	2.6	2.6	2.5	-	Olefinic hydrogens in ester (Madankar et al., 2013)
3.96	dt	0.8	1	1.6	158.58, 4.88	...-Ar-O-CH ₂ -CH ₂ -.....-O-CH ₂ -CH ₂ -O-H
3.66	m	12.9	12.8	17.3	-	Terminal Methoxy proton (Tariq et al., 2011) Oxy-ethylene protons -(O-CH ₂ -CH ₂)-
3.46	s	1.3	1.3	2.2	-	Terminal HO- of ethene
2.76	t	0.4	0.5	0.4	2.75	di-vinyl methylene protons (due to presence of Methyl Linoleate)(SCIENTIFIC)
2.3	t	4.7	4.8	4	7.57	α- CH ₂ proton (Tariq et al., 2011)
2	dq	5	4.5	4.6	22.85, 7.02	Allylic hydrogens (SCIENTIFIC)
1.95, 1.88, 1.93	S (broad)	2.5	2.9	4	-	water
1.68	s	0.4	0.5	0.9	-	(CH ₃) ₃ CH ₂ -
1.6	t	4.8	4.8	4.1	6.79	β- carbonyl protons (Tariq et al., 2011)
1.28	m	55	55	47.6	-	Methylene protons (Tariq et al., 2011)
0.9	t	7	7	5.8	6.7	Terminal methyl protons (Tariq et al., 2011)
0.7	S	1.9	2	3.6	-	Terminal methyl proton

4.5 Thermogravimetric analysis (TGA)

This section has studied the thermal behavior of neat palm biodiesel and emulsified biodiesel. This method is based on the principle of variation of sample mass as function of time or temperature. Onset temperature (T_{on}) and offset temperature (T_{off}) are most important parameters of TGA analysis (Jain & Sharma, 2012). T_{on} is used to indicate thermal degradation resistance ability of biodiesel. This is determined by extrapolating the horizontal baseline at 1% degradation. The intercept of this line with tangent to the downward portion of the weight curve is defined as T_{on} . After the sample is completely burnt then TGA curve flattens out. The intercept of the extrapolation on this flattened line and the tangent to the downward portion is called as T_{off} . **Figure 4.6**, shows onset and offset temperature calculation of single step (**Figure 4.6(a)**) and multi-step (**Figure 4.6(b)**) decomposition of the samples. **Figure 4.7** shows the TG and DTG curves of diesel, neat biodiesel and emulsified biodiesels. From **Figure 4.7(a)**, it can be seen that for diesel there are 3 onsets and offset points. For neat biodiesel, there is one set of onset and offset temperature. For emulsified there are two sets of onset and off set temperatures. With increase in water content in the sample, onset temperature also increases in emulsified biodiesel. However, onset temperature of MTX-3 is decreased compared to MTX-2. The reason for this phenomenon may be due to higher instability, which promotes decomposition to starts at lower temperature. Due to higher amount of water inside MTX-3, the water droplets goes down due to gravitation and the upper layer is more with B-100. Therefore the decomposition starts quicker than that of MTX-2.

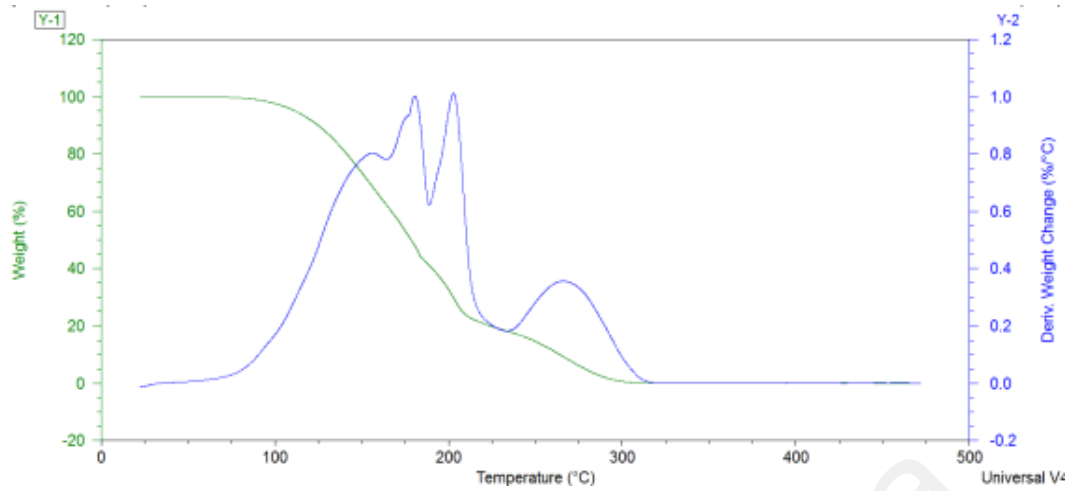


(a)

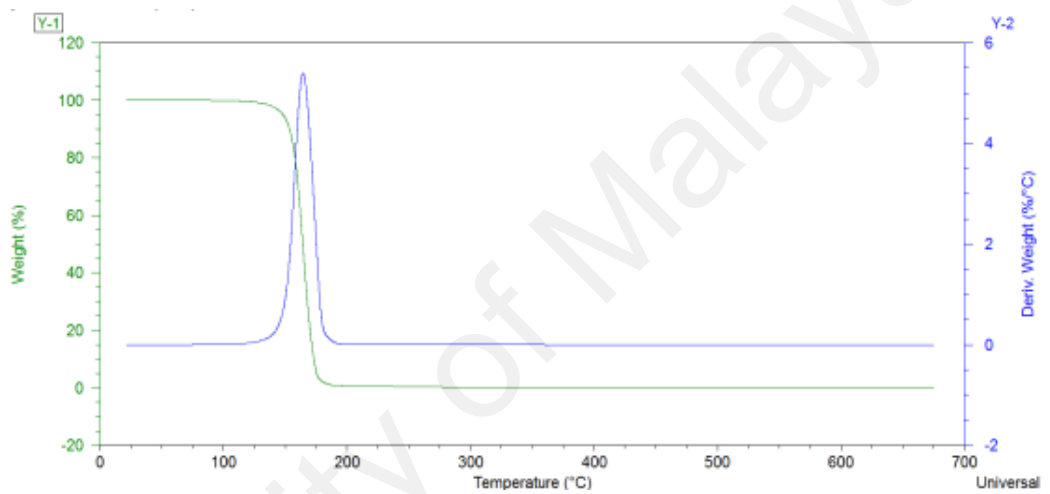


(b)

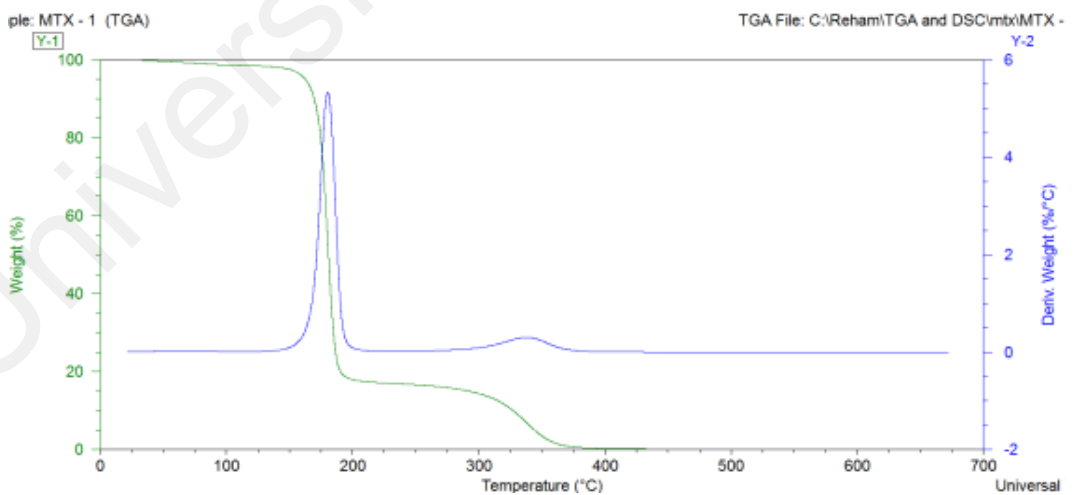
Figure 4.6: Onset and offset temperatures of (a) neat biodiesel and (b) MTX-1 biodiesel emulsion during thermal decomposition



(a)

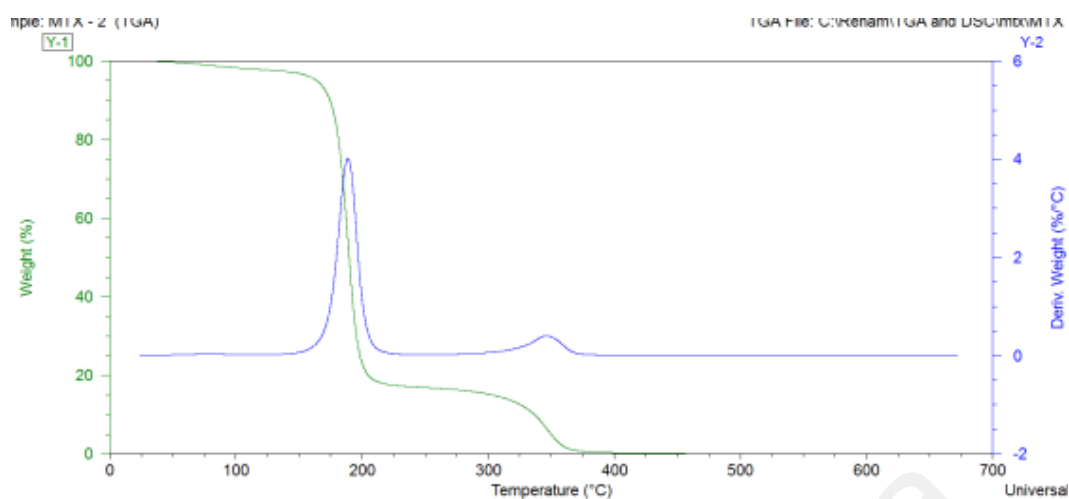


(b)

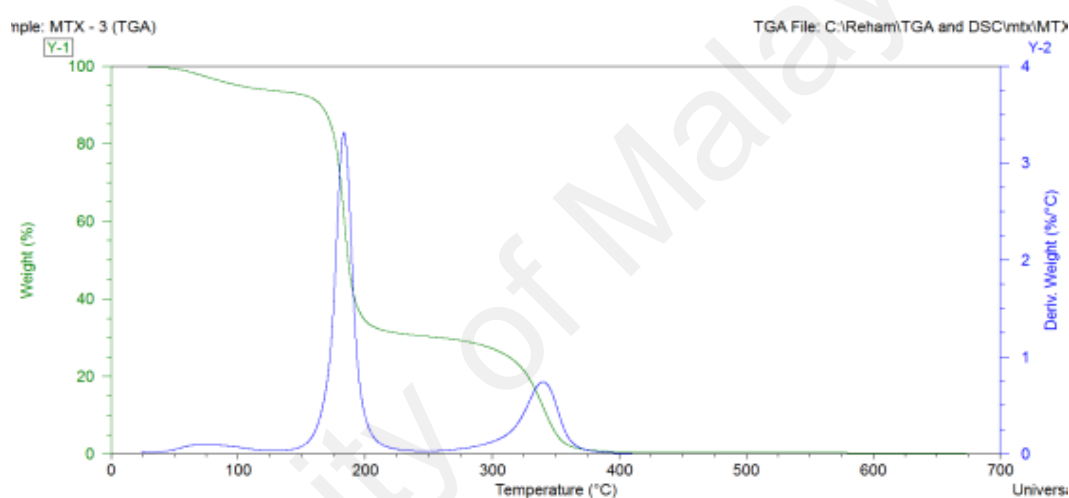


(c)

Figure 4.7: Weight change with respect to temperature and derivative weight change with respect to temperature are provided for (a) Diesel, (b) B-100 (Palm biodiesel) (c) MTX-1, (d) MTX-2 and (e) MTX-3.



(d)



(e)

Figure 4.7: Continued

From **Table 4.6**, it can be seen that volatility is present in emulsified biodiesels. For emulsion samples, water and ethanol decompose in this stage. As higher the water concentration higher is the amount of co-surfactant, the weight loss in this stage changes accordingly. **Table 4.6** provides the numerical value of weight loss in each decomposed stage. The changes in weight occurred due to formation and breaking of physical and chemical bonds of the sample (Wan Nik et al., 2005). In neat biodiesel, the decomposition is due to pyrolysis of methyl esters (Jain & Sharma, 2012). Therefore, in biodiesel emulsions, first sharp decomposition is due to pyrolysis of methyl ester. The second decomposition is due to surfactant (Ttiton X-100) as this is the only component left to

decompose. MTX-1 and MTX-2 curves are similar with slight deviation but MTX-3 gives higher deviation. The 1st and 2nd weight loss of MTX-1 and MTX-2 is similar. However, 2nd weight loss of MTX-3 is much higher than MTX-1 and MTX-2 (as shown in **Figure 8**). This is due to presence of higher amount of surfactant in MTX-3 compared to other two emulsions. **Table 4.6** shows that MTX-2 gives higher decomposition temperature and therefore it is more thermodynamically stable than other samples. However, diesel has lowest decomposition temperature pointing its weaker thermal stability.

Table 4.6: TG and DTG analysis of Diesel, Biodiesel and emulsified biodiesel

Parameters	B-100	MTX-1	MTX-2	MTX-3	Diesel
First Onset temperature (°C)	155	172	178	173	127.7
First offset temperature (°C)	173	186	197	191.6	-
Second Onset temperature (°C)	-	309	324	319	182.95
Second offset temperature (°C)	-	358	361	356	-
Third onset temperature (°C)	-	-	-	-	249
Third offset temperature (°C)	-	-	-	-	294.7
Volatiles (% mg per mg)	None found	1.62	2.141	6.273	Not found
1st weight loss (% mg per mg)	99.67	81.85	80.88	63.67	56.86
2nd weight loss (% mg per mg)	-	16.56	16.54	29.62	24.51
3rd weight loss (% mg per mg)	-	-	-	-	18.85
Residue (% mg per mg)	~0	0.1008	0.1158	0.2509	0.02

Figure 4.8, DTG with time graph, provides the time frame for decompositions. Maximum DTG is attained at same time in B-100 and MTX-1. MTX-2 attained its maximum DTG few minutes after B-100. One stage decomposition process of B-100 took least time to fully decompose than any other sample. With increase in water concentration, time to decompose full sample has increased.

Figure 4.9 shows that the rate of weight changes. Rate of weight change of B-100 is higher than emulsified biodiesels. However, for emulsified biodiesel, with the increase in water concentration the rate of 1st weight change decreases but 2nd weight change increases with respect to time and temperature. The residue is higher with the increase in water concentration. Therefore, rate of weight change depends on the quantity of material present in the sample. Higher the quantity of the sample more is the rate of its decomposition.

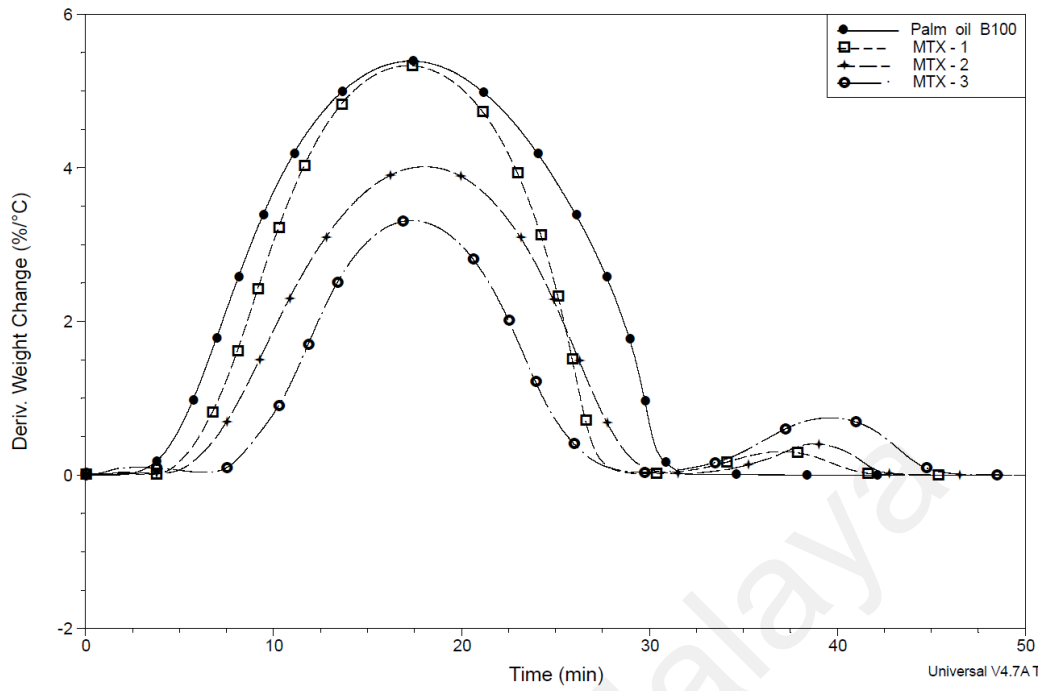


Figure 4.8: Derivative of weight change with respect to temperature vs time of neat biodiesel and emulsified biodiesel

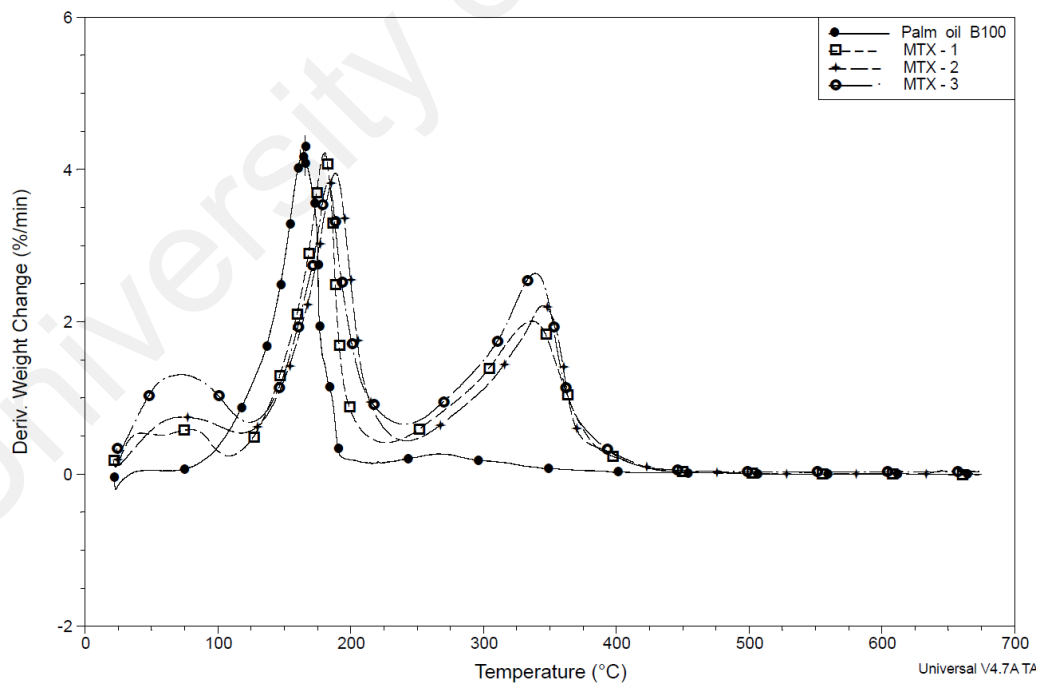


Figure 4.9: Change of weight with respect to time vs temperature of B-100 and emulsified biodiesel samples

4.6 Differential scanning calorimetry (DSC) analysis:

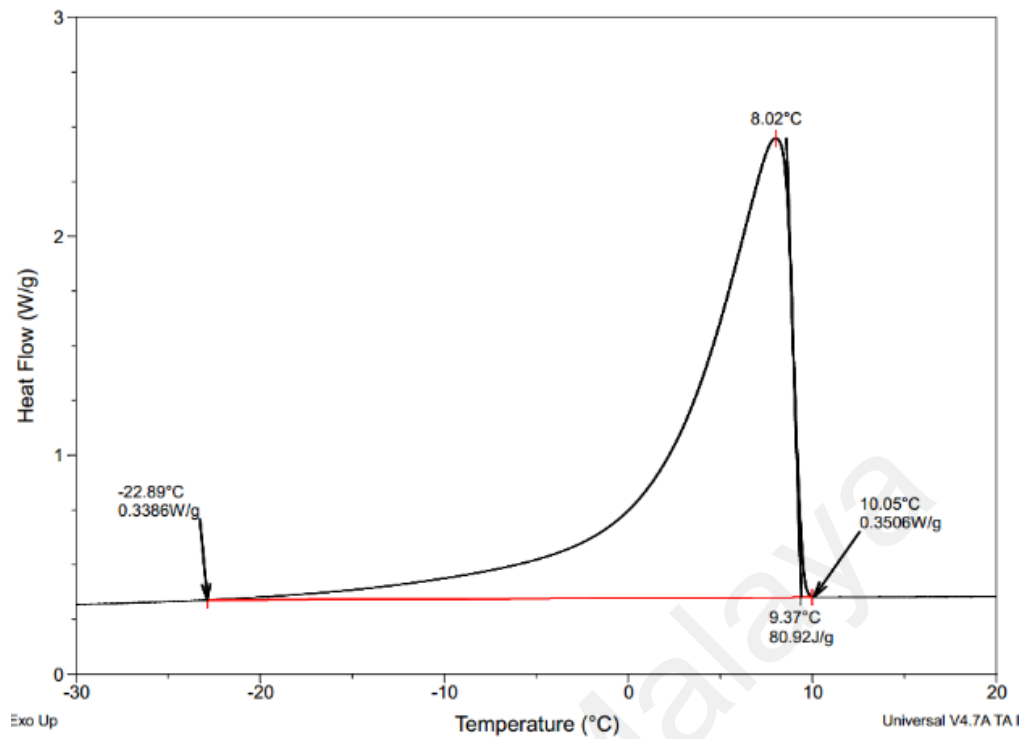
Differential scanning calorimetry analysis is done to identify exothermic and endothermic reactions, corresponding crystallization and melting points and magnitude of heat fluxes. **Figure 4.10**, shows two curves of B-100 (a) and (b), transition peaks pointing upward are exothermic and peaks pointing downward are endothermic. In appendix DSC curves of emulsified samples are provided. Exothermic curve indicates crystallization from liquid to solid phase and endothermic curve indicated the absorption of energy for melting transitions. Onset temperatures are calculated for each transition. Onset temperature is the point of intersection of lines drawn tangent to the base line and the point of sharpest increase in the slope of transition peak. And the points presenting maximum change in heat flow of the transition peaks are melting and/ or crystallization temperature (Dunn, 2012).

Table 4.7, presents the results of significant parameters during DSC analysis. From **Table 4.7**, it is seen that, highest melting point is achieved by MTX-2. Onset of melting point is higher in MTX-2 compared to B-100 and diesel. However, MTX-3 has onset of melting point much lower than neat biodiesel but higher than that of diesel. Crystallization temperature is improved with the addition of water. Reduction of onset temperature of crystallization in emulsion is due to increased amount of solute present in the solution. This is explained by freezing-point depression theory, where Hildebrand equation for ideal solutions states that, a reduction in the concentration of solute results in increase in the crystallization temperature (Garcia-Perez et al., 2010). Therefore, reduction of Methyl ester concentration due to addition of emulsifier and water, the onset of crystallization temperature is reduced. MTX-2 has lowest crystallization temperature and highest melting temperature.

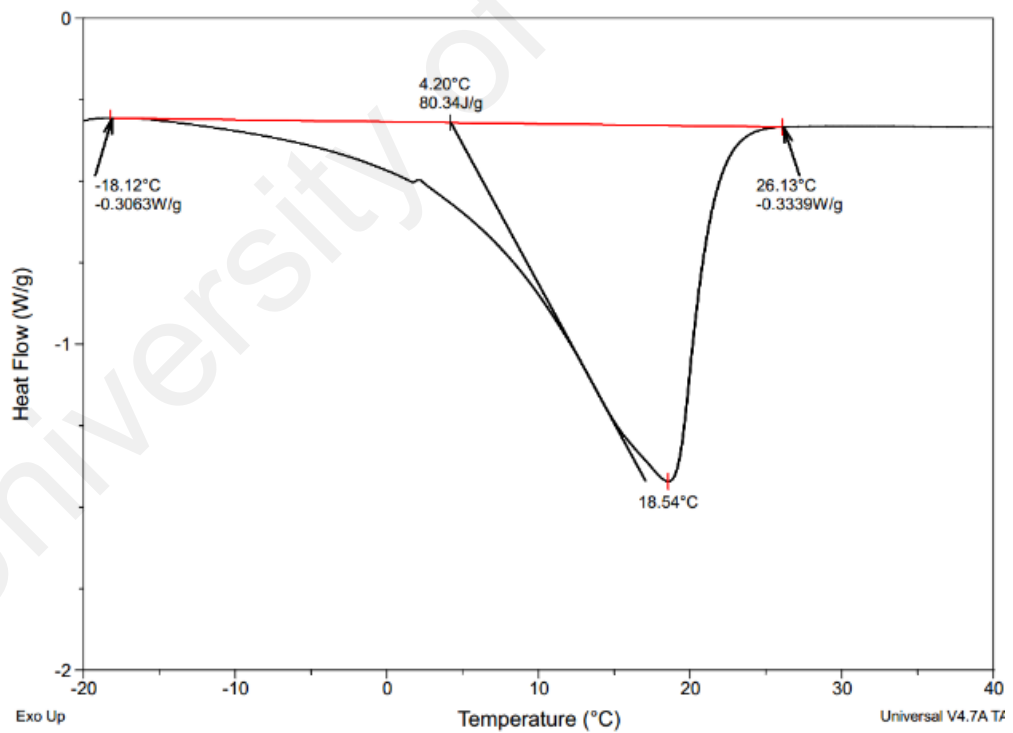
Table 4.7: Thermal characteristics (DSC) of neat and emulsified palm biodiesels

Parameters	B-100	MTX-1	MTX-2	MTX-3	Diesel
Melting temperature (T_m) (°C)	18.54	18.28	19.2	17.85	-8.35
Onset temperature for melting (°C)	4.17	4.55	4.41	-0.52	-39
Enthalpy of melting (ΔH) (Jg ⁻¹)	80.86	62.58	62.39	28.35	23
Temperature range for melting (°C)	-18.17 to -28.71	-16.99 to -26.21	-16.42 to -28.51	-16.42 to -22.63	-58 to -19.7
Heat flow range for melting (Wg ⁻¹)	-0.3064 to -0.3319	-0.2920 to -0.2799	-0.2846 to -0.2720	-0.1184 to -0.1196	-0.26 to -0.28
Crystallization temperature (T_c) (°C)	8.02	6.97	6.53	7.95	-16.5
Onset temperature for crystallization (°C)	9.38	8.75	8.68	8.49	1.67
Enthalpy of crystallization (ΔH) (Jg ⁻¹)	79.73	59.09	58.49	21.16	21.05
Temperature range for crystallization (°C)	-12.56 to -18.75	-18.14 to -29.65	-10.23 to -20.89	-11.03 to -11.68	-58 to -12.7
Heat flow range for crystallization (Wg ⁻¹)	0.3515 to 0.3587	0.2907 to 0.2830	0.2838 to 0.2934	0.1673 to 0.2032	0.28 to 0.29

Fuel property analysis shows that MTX-2 gives the better characteristics than other emulsified biodiesel for its negligible changes in viscosity, calorific value and improvement in oxidation stability as well as thermal stability. Wan Nik et al. (2005) improved biodiesel's thermal stability by addition of additives (Irgalube F10). According to their findings, after addition of 2% of this additive, onset temperature is increased by 10.66%. This additive is used as anti-oxidants. Jain and Sharma (2012) also used anti-oxidants to improve onset temperature of thermal decomposition of biodiesel. After addition of 300 ppm additives to biodiesel, the onset temperature has increased from 128 °C to 170 °C. Higher amount of additive usage improved their biodiesel's onset temperature more. However, in this study, TGA analysis shows that, addition of only 1 % water increased the onset temperature by 11% and 2% water addition increased the onset temperature by 15%.



(a)



(b)

Figure 4.10: DSC curve analysis of Palm biodiesel at $10\text{ }^{\circ}\text{C min}^{-1}$ heating rate for (a) cooling scans (b) heating scans.

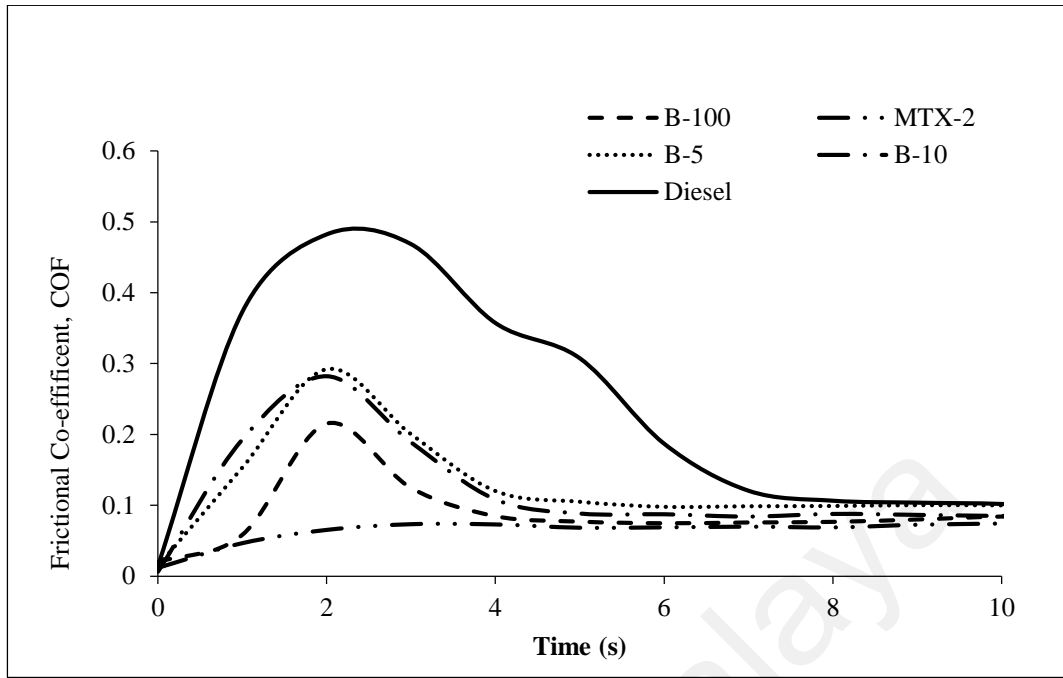
4.7 Friction and wear analysis.

Friction and wear analysis is performed to analyze the lubricating characteristics of emulsified biodiesel.

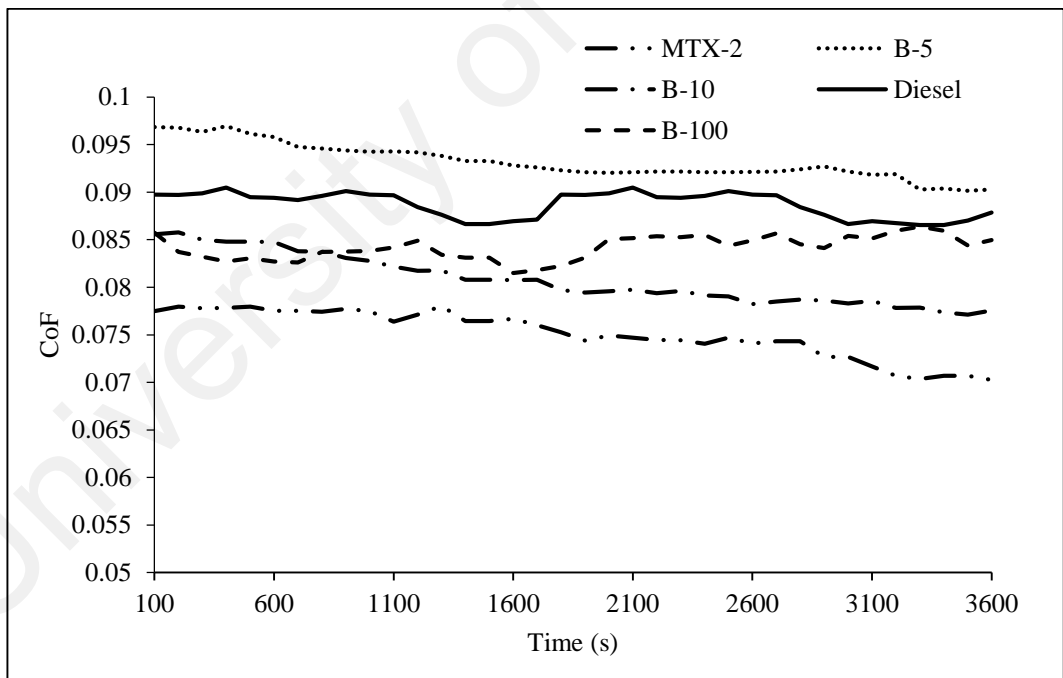
4.7.1 CoF Analysis

Figure 4.11 shows the co-efficient of friction (CoF) of fuel samples with time. **Figure 4.11 (a)**, shows results of run-in period. Run-in –period condition is usually at the starting of each test when friction is unstable (Mosarof et al., 2016). Each fuel sample shows a bump in the COF vs time graph at the start of the test. To change from rest to motion first the friction occurs is due to static friction after that during full motion the friction is due to dynamic or kinetic friction. Generally, static friction is higher than dynamic friction. Therefore, all fuels are displayed of higher CoF at the first few seconds are due to static friction. Moreover, the contact surfaces of the test balls become smoother and noticeable asperities are flattened with an increase the running time during the friction test. This may consider as the transition of unsteady state to steady state level (Fazal et al., 2013). In all samples (except MTX-2) the unsteady state CoF increased sharply at higher value for first few seconds and then decreased gradually and becomes smoother and stable. However, the friction of MTX-2 at the start is not that high rather a smooth rise is visible and after few seconds the raised value became constant throughout the test. In unsteady state, lowest CoF was found with MTX-2 and second lowest was found with B-100. This result can be explained due to the absorption of ester molecules of biodiesel in the metal contact surfaces. These absorbed ester molecules act as surfactants for the solid contact surface (Fazal et al., 2013). Therefore, presence of surfactant and co-surfactant in MTX-2 might enhance this lower friction behavior. This also explains reason of the smooth transition of CoF of MTX-2 from unsteady to steady state.

Figure 4.11 (b), shows the steady state value of CoF for all fuel samples over 3600 s duration. Mild fluctuation of value of CoF is seen in MTX-2, BTX-5 and BTX-10. High fluctuation in value of CoF of diesel can be observed from **Figure 4.11(b)**. B-100 gives the very smooth steadier CoF value within increasing the time compared to that of other samples. BTX-5 has highest steady state CoF compared to other samples. CoF of BTX-10 is similar to that of MTX-2. From **Figure 4.11(b)** it can be seen that; CoF decreases with an increasing the concentration of MTX-2 in diesel fuel. Average CoF values of all samples are provided in **Figure 4.12**. Average CoF of diesel is 17% lower than that of BTX-5. Average COF value of MTX-2 is lower compared to diesel, B-100, BTX-5 and BTX-10. When CoF varies substantially wear will be higher (Nohava et al., 2016). That is been proved by highest WSD from diesel. However, the average value of B-100 is 15.3% higher than MTX-2.



(a)



(b)

Figure 4.11: Friction co-efficient behaviour with respect to time in (a) run-in-period and (b) steady state condition

4.7.2 Wear scar diameter analysis

Figure 4.13 shows the wear scar diameter (WSD) of all fuel samples. WSD indicates the severity of wear caused by the fuel. Smaller WSD generally indicates less wear (Syahrullail et al., 2013). WSD of fuel increases with an increase in wear load, this is because of increase in contact pressure between the metal surfaces, increase the formation of oxidation at the contact surface. Hence the tribological characteristics of biodiesel deteriorate. This deterioration is also caused by the removal of the metallic soap film generated at high load (Bhattacharya et al., 1990; Jayadas et al., 2007). The higher WSD was found with diesel fuel compared to other fuel samples. B-100 caused smallest WSD compared to diesel and emulsion fuel blends. The presence of ester groups in pure biodiesel may be the main reason of lower WSD of pure biodiesel. Increased the amount of ester molecules which can enhance the bonding of molecules. In addition, presence of higher amount of oxygen content in biodiesel, which helps to reduce the wear and friction between the contact surfaces (Habibullah et al., 2015). Length of fatty acid chain plays an important role in forming a lubricant film between the metal contact surfaces. This film works as a protective film and reduces thermal energy in sliding contact surfaces and it can be enhanced better lubrication performance (Havet et al., 2001; Hu et al., 2005; Knothe & Steidley, 2005). WSD of MTX-2 is 25% lower than the diesel fuel.

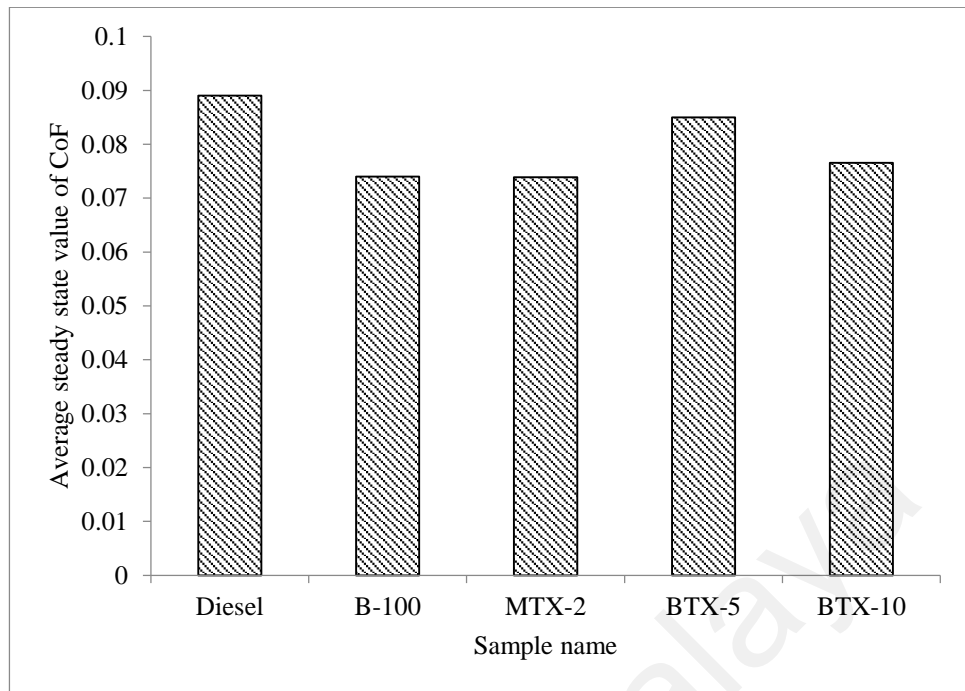


Figure 4.12: Average CoF value of samples during steady state condition

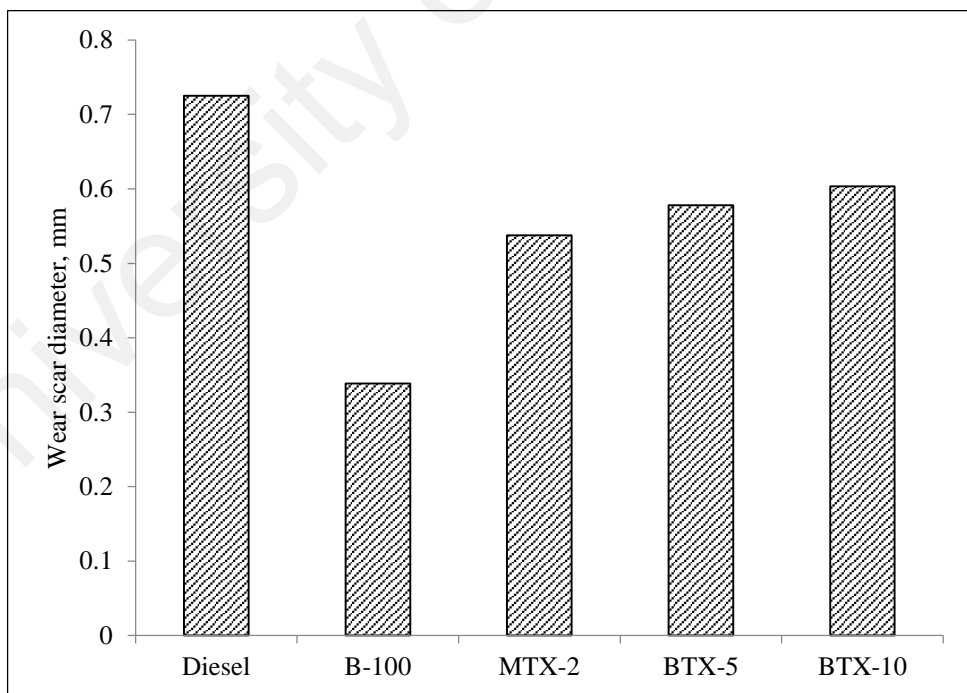


Figure 4.13: Wear scar diameter of different fuel samples

4.7.3 SEM and EDX Analysis

Figure 4.14 shows SEM (topographic images) analyzer is used to examine the worn scar surfaces of the tested steel balls. Elemental analysis on the worn scar surface of the tested steel ball has been done by Energy-dispersive X-ray spectroscopy (EDX). It was seen that; MTX-2 showed lower worn scar surfaces are compared to diesel fuel. The higher worn scar surface area found with diesel fuel than other fuel samples. This is due to the presence of ester molecules in palm biodiesel mainly MTX-2 based diesel fuel, which improved the lubrication performance and reduced the worn scar surfaces. It is reported that the ester molecules in palm biodiesel could generate a monolayer lubricating film on the metal rubbing surfaces and enhance the better lubricity of the biodiesel (Habibullah et al., 2015). Moreover, the higher oxygen content and composition of fatty acid contained in MTX-2 blends could form inorganic oxides such as FeS and Fe₂O₃ by the formation of lubricating film (Mosarof et al., 2016). It was observed that the metal surface of the tested balls for each fuel was damaged by the adhesive wear because worn surface was greater than 20 µm. However, some worn surface showed radial, mild and regular scratches in resulting that caused by abrasive wear (Sperring & Nowell, 2005). Some fracture was found with B100, BTX-5 and BTX-10, which causes the fatigue, wear in the metal contact surface. Wear debris are presented in the worn scar surface of diesel and BTX-10. It can be seen that; the worn surfaces for diesel, MTX-2, BTX-5, BTX-10 and B100 were damaged by adhesive wear. The presence of black spots on the worn scar surfaces of the ball tested in B100, MTX-2, BTX-5 and BTX-10 which reflected by the oxidative corrosion and then aggravated the corrosive wear on the metal contact surfaces. During oxidation process, the various types of peroxides and acids were created and adversely effect on the lubricity of the fuel (Bhale et al., 2008).

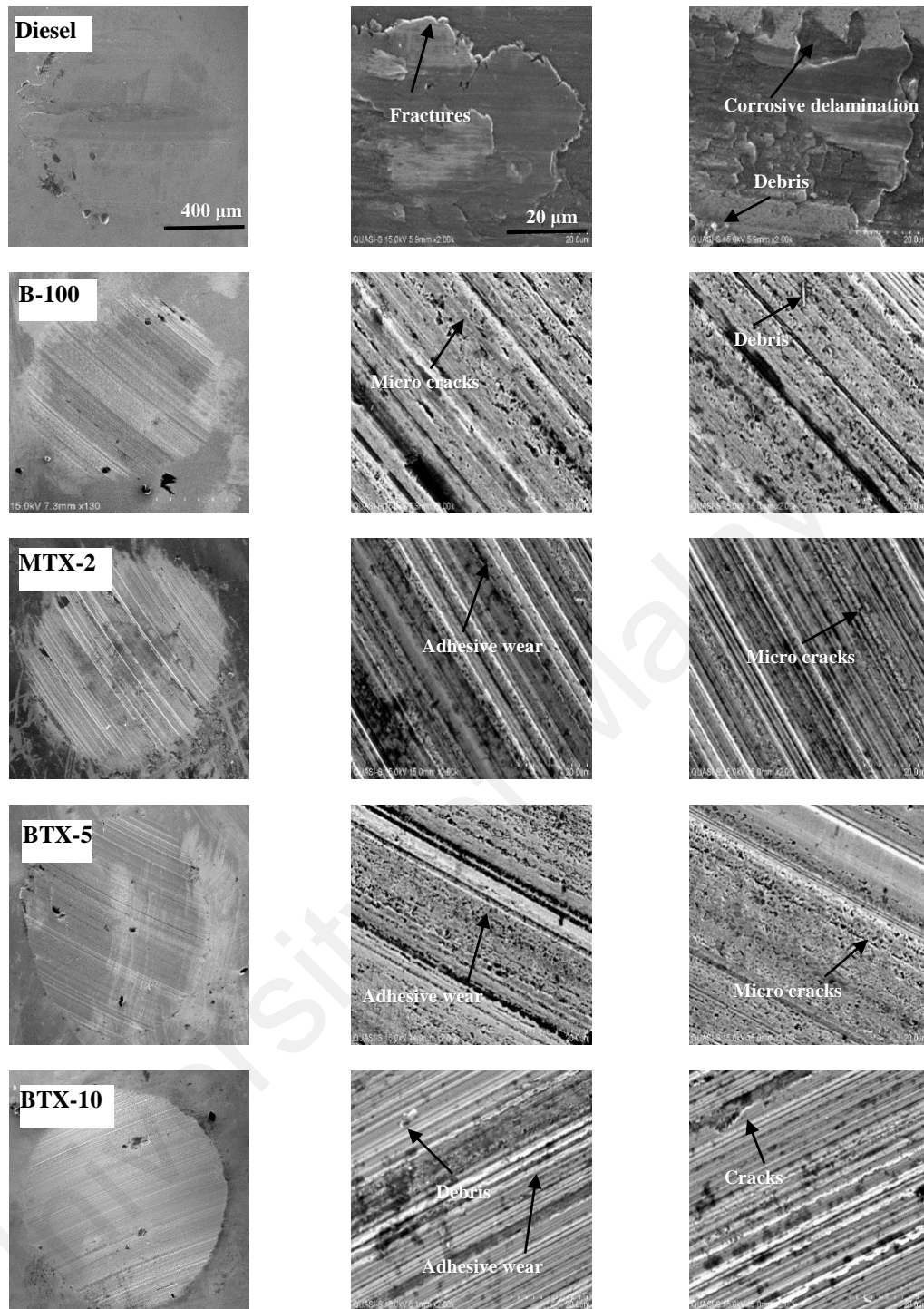


Figure 4.14: SEM analysis of the wear areas of steel ball

4.7.4 Elemental analysis

Figure 4.15 shows the element abundance at the wear area for B-100, MTX-2, BTX-5, BTX-10 and diesel. Carbon, chromium and ferrous are mostly comes from the steel ball. Oxygen comes from biodiesel and represents the amount of oxidation occurred in the affected area. MTX-2 has a very low value of oxygen content compared to other samples. B-100 has highest oxygen level compared to that of other samples. BTX-10 has 2.2% lower oxygen content compared to BTX-5. Oxygen content of MTX-2 has reduced by 60% and 27% compared to B-100 and diesel respectively. Therefore, addition of water in biodiesel through emulsification reduces oxidation and can work as anti-oxidant.

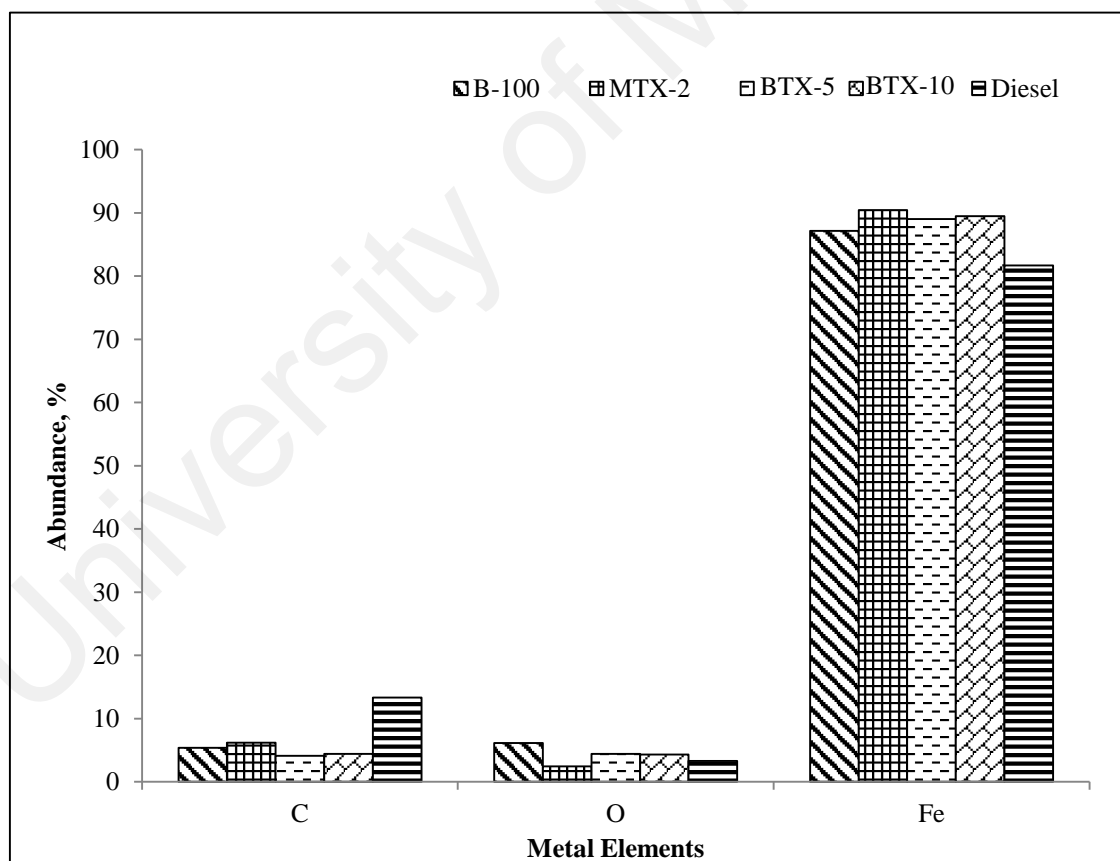


Figure 4.15: Element abundance in percentage at the wear surface of the steel ball for each sample

Friction and wear analysis shows that MTX-2 has lower WSD compared to diesel but higher WSD compared to B-100. However, frictional co-efficient is improved when water is added to B-100. This can be explained by the phenomenon of fluctuating value of CoF. Value of CoF of MTX-2 is more fluctuating than B-100. Therefore, wear is high in MTX-2 compared to B-100. Elemental analysis in the wear area shows low abundance of oxygen in MTX-2 compared to that of B-100, BTX-5 and BTX-10. Therefore, wear due to oxidation is very low when water is added to biodiesel compared to neat biodiesel. Therefore, from the studies it shows that water may help to increase oxidation stability when added to biodiesel. This will improve the quality of biodiesel as well as reduce the cost of using expensive anti-oxidants.

CHAPTER 5: CONCLUSIONS AND RECOMMENDATION

5.1 Conclusion

The main objective of this research endeavor is to study the potential of emulsified fuel using palm oil as a promising biodiesel feedstock which is easily accessible in many parts of the world. Series of experiment were sequentially conducted in this research to characterize the physical and chemical properties of palm biodiesel emulsion such as kinematic viscosity, density, calorific value and oxidation stability. To explore the chemical bond characteristics FTIR. Thermal property of emulsified biodiesel is analyzed and compare with that of biodiesel fuel using thermogravimetric analysis. Finally, lubricating properties of emulsified biodiesel is explored and analyzed. Based on these research work, the following conclusion could be drawn:

1. Maximum physicochemical properties of all modified biodiesel agree with ASTM and EN standard.
2. Emulsification has significantly improved the oxidation stability and thermal stability of palm biodiesel. Oxidation stability of MTX-2 is 102% higher than diesel and 27% higher than palm biodiesel. MTX-3 has 110% and 32% higher oxidation stability time from diesel and biodiesel respectively. From TGA it is found that, addition of only 1 % water increased the onset temperature by 11% and 2% water addition increased the onset temperature by 15% compared to that of neat biodiesel
3. MTX-2 has lower WSD compared to diesel but higher WSD compared to B-100. Wear due to oxidation is lower in emulsified biodiesel than that of neat diesel and neat biodiesel. The CoF and worn scar surfaces of MTX-2 have found lower than diesel and neat biodiesel.

In conclusion, palm biodiesel emulsification has improved the oxidation and thermal property compared to neat biodiesel and diesel. In this study 2% water concentration

emulsion with TritonX-100 gave the best fuel properties compared to other emulsified fuel.

5.2 Recommendation for future work

Following recommendations for the future work can be suggested:

This study has been carried out in fuel property, thermal and oxidation stability and lubrication characteristics of fuel emulsion. For future work in this area, researcher may study on improvement of viscosity of emulsified biodiesel and can study further to improve CoF to attain steady value of CoF in biodiesel emulsion which is important to reduce the friction. Besides, engine tests can be done to check performance, combustion and emission of emulsified fuel.

University of Malaya

REFERENCES

- (IEA), I. E. A. (2011). Technology Roadmaps - Biofuels for Transport, from http://www.iea.org/publications/free_new_Desc.asp
- Abu-Zaid, M. (2004). Performance of single cylinder, direct injection Diesel engine using water fuel emulsions. *Energy Conversion and Management*, 45(5), 697-705.
- Agriculture, U. S. D. o. (2013). Palm oil: world supply and distribution
- Alahmer, A., Yamin, J., Sakhrieh, A., & Hamdan, M. A. (2010). Engine performance using emulsified diesel fuel. *Energy Conversion and Management*, 51(8), 1708-1713.
- Ambrosone, L., Mosca, M., & Ceglie, A. (2007). Impact of edible surfactants on the oxidation of olive oil in water-in-oil emulsions. *Food Hydrocolloids*, 21(7), 1163-1171.
- Anand, K., Sharma, R., & Mehta, P. S. (2011). Experimental investigations on combustion, performance and emissions characteristics of neat karanja biodiesel and its methanol blend in a diesel engine. *biomass and bioenergy*, 35(1), 533-541.
- Archard, J., & Hirst, W. (1956). *The wear of metals under unlubricated conditions*. Paper presented at the Proceedings of the Royal Society of London A: Mathematical, Physical and Engineering Sciences.
- Armas, O., Hernández, J. J., & Cárdenas, M. D. (2006). Reduction of diesel smoke opacity from vegetable oil methyl esters during transient operation. *Fuel*, 85(17-18), 2427-2438.
- Atadashi, I., Aroua, M., Abdul Aziz, A., & Sulaiman, N. (2012). Production of biodiesel using high free fatty acid feedstocks. *Renewable and Sustainable Energy Reviews*, 16(5), 3275-3285.
- Atadashi, I., Aroua, M., & Aziz, A. A. (2011). Biodiesel separation and purification: a review. *Renewable Energy*, 36(2), 437-443.
- Atmanlı, A., İleri, E., & Yüksel, B. (2014). Experimental investigation of engine performance and exhaust emissions of a diesel engine fueled with diesel-n-butanol-vegetable oil blends. *Energy Conversion and Management*, 81(0), 312-321.
- Atwood, S. A., Van Citters, D. W., Patten, E. W., Furmanski, J., Ries, M. D., & Pruitt, L. A. (2011). Tradeoffs amongst fatigue, wear, and oxidation resistance of cross-linked ultra-high molecular weight polyethylene. *Journal of the Mechanical Behavior of Biomedical Materials*, 4(7), 1033-1045.
- Balaji, G., & Cheralathan, M. (2013). Experimental investigation to reduce emission of CI (compression ignition) engine fuelled with methyl ester of cottonseed oil using antioxidant. *International Journal of Ambient Energy*, 35(1), 13-19.

- Basha, S. A., Gopal, K. R., & Jebaraj, S. (2009). A review on biodiesel production, combustion, emissions and performance. *Renewable and Sustainable Energy Reviews*, 13(6–7), 1628-1634.
- Bhale, P. V., Deshpande, N., & Thombre, S. (2008). Simulation of wear characteristics of cylinder liner–ring combination with diesel and biodiesel. *Society of Automotive Engineers*.
- Bhattacharya, A., Singh, T., Verma, V. K., & Nakayama, K. (1990). The role of certain substituted 2-amino-benzothiazolylbenzoylthiocarbamides as additives in extreme pressure lubrication of steel bearing balls. *Wear*, 136(2), 345-357.
- Bhimani, S., Alvarado, J. L., Annamalai, K., & Marsh, C. (2013). Emission characteristics of methanol-in-canola oil emulsions in a combustion chamber. *Fuel*, 113(0), 97-106.
- Bhushan, B. (2000). *Modern tribology handbook, two volume set*: CRC press.
- Can, Ö. (2014). Combustion characteristics, performance and exhaust emissions of a diesel engine fueled with a waste cooking oil biodiesel mixture. *Energy Conversion and Management*, 87, 676-686.
- Çaynak, S., Gürü, M., Biçer, A., Keskin, A., & İcingür, Y. (2009). Biodiesel production from pomace oil and improvement of its properties with synthetic manganese additive. *Fuel*, 88(3), 534-538.
- Chen, G., & Tao, D. (2005). An experimental study of stability of oil–water emulsion. *Fuel Processing Technology*, 86(5), 499-508.
- Clausse, D., Pezron, I., & Komunjer, L. (1999). Stability of W/O and W/O/W emulsions as a result of partial solidification. *Colloids and Surfaces A: Physicochemical and Engineering Aspects*, 152(1–2), 23-29.
- Crookes, R. J., Kiannejad, F., & Nazha, M. A. A. (1997). Systematic assessment of combustion characteristics of biofuels and emulsions with water for use as diesel engine fuels. *Energy Conversion and Management*, 38(15–17), 1785-1795.
- D.T. Wasa, A.D. Nikolou, & Ainetti, F. (2004). Texture and stability of emulsions and suspensions—role of oscillatory structural forces. *Adv Colloids Interface Sci*, 187-195.
- Debnath, B. K., Sahoo, N., & Saha, U. K. (2013). Adjusting the operating characteristics to improve the performance of an emulsified palm oil methyl ester run diesel engine. *Energy Conversion and Management*, 69(0), 191-198.
- Demirbas, A. (2009a). Biorefineries: Current activities and future developments. *Energy Conversion and Management*, 50(11), 2782-2801.
- Demirbas, A. (2009b). Political, economic and environmental impacts of biofuels: A review. *Applied Energy*, 86, Supplement 1, S108-S117.

- Denkov, N. D., Tcholakova, S., Ivanov, I. B., & Campbell, B. (2002). Methods for evaluation of emulsion stability at a single drop level. *Third World Congress on Emulsions, Lyon*.
- Dhar, A., Kevin, R., & Agarwal, A. K. (2012). Production of biodiesel from high-FFA neem oil and its performance, emission and combustion characterization in a single cylinder DIC engine. *Fuel Processing Technology, 97*, 118-129.
- Dong, S., Tu, J., & Zhang, X. (2001). An investigation of the sliding wear behavior of Cu-matrix composite reinforced by carbon nanotubes. *Materials Science and Engineering: A, 313*(1), 83-87.
- Dunn, R. O. (2012). *Effects of high-melting methyl esters on crystallization properties of fatty acid methyl ester mixtures*. Paper presented at the American Society of Agricultural and Biological Engineers.
- Fazal, M. A., Haseeb, A. S. M. A., & Masjuki, H. H. (2013). Investigation of friction and wear characteristics of palm biodiesel. *Energy Conversion and Management, 67*, 251-256.
- Fernando, S., & Hanna, M. (2005). Phase behavior of the ethanol-biodiesel-diesel micro-emulsion system. *Transactions of the American Society of Agricultural Engineers, 48*(3), 903-908.
- Fingas, M., & Fieldhouse, B. (2003). Studies of the formation process of water-in-oil emulsions. *Marine Pollution Bulletin, 47*(9-12), 369-396.
- Foo, K. Y., & Hameed, B. H. (2009). Utilization of biodiesel waste as a renewable resource for activated carbon: Application to environmental problems. *Renewable and Sustainable Energy Reviews, 13*(9), 2495-2504.
- Friberg, S. E., Young, T., Mackay, R. A., Oliver, J., & Breton, M. (1995). Evaporation from a microemulsion in the water-aerosol OT-cyclohexanone system. *Colloids and Surfaces A: Physicochemical and Engineering Aspects, 100*(0), 83-92.
- Garcia-Perez, M., Adams, T. T., Goodrum, J. W., Das, K. C., & Geller, D. P. (2010). DSC studies to evaluate the impact of bio-oil on cold flow properties and oxidation stability of bio-diesel. *Bioresource Technology, 101*(15), 6219-6224.
- Griffin, W. C. (1949a). Classification of surface-active agents by "HLB". *Journal of COSMETIC SCIENCE, 1*, 311-326.
- Griffin, W. C. (1949b). Classification of surface-active agents by HLB. *J Soc Cosmet Chem, 1*, 311-320.
- Gülseren, İ., & Corredig, M. (2014). Interactions between polyglycerol polyricinoleate (PGPR) and pectins at the oil-water interface and their influence on the stability of water-in-oil emulsions. *Food Hydrocolloids, 34*(0), 154-160.
- Habibullah, M., Masjuki, H., Kalam, M., Zulkifli, N., Masum, B., Arslan, A., & Gulzar, M. (2015). Friction and wear characteristics of Calophyllum inophyllum biodiesel. *Industrial Crops and Products, 76*, 188-197.

- Habibullah, M., Masjuki, H. H., Kalam, M. A., Zulkifli, N. W. M., Masum, B. M., Arslan, A., & Gulzar, M. (2015). Friction and wear characteristics of Calophyllum inophyllum biodiesel. *Industrial Crops and Products*, 76, 188-197.
- Hagos, F. Y., Aziz, A. R. A., & Tan, I. M. (2011). *Water-in-diesel emulsion and its micro-explosion phenomenon-review*. Paper presented at the 2011 IEEE 3rd International Conference on Communication Software and Networks, ICCSN 2011.
- Hans-Jurgen Butt, K. G., Michael Kappl. (2013). *Physics and Chemistry of Interfaces, 3rd Edition*: WILEY-VCH.
- Havet, L., Blouet, J., Robbe Valloire, F., Brasseur, E., & Slomka, D. (2001). Tribological characteristics of some environmentally friendly lubricants. *Wear*, 248(1–2), 140-146.
- Hoekman, S. K., & Robbins, C. (2012). Review of the effects of biodiesel on NOx emissions. *Fuel Processing Technology*, 96(0), 237-249.
- Hu, J., Du, Z., Li, C., & Min, E. (2005). Study on the lubrication properties of biodiesel as fuel lubricity enhancers. *Fuel*, 84(12–13), 1601-1606.
- Husnawan, M., Masjuki, H. H., Mahlia, T. M. I., & Saifullah, M. G. (2009). Thermal analysis of cylinder head carbon deposits from single cylinder diesel engine fueled by palm oil–diesel fuel emulsions. *Applied Energy*, 86(10), 2107-2113.
- IER. (2015). Global consumption of fossil fuel countries to increase. Retrieved from <http://instituteeforenergyresearch.org/analysis/global-consumption-of-fossil-fuels-continues-to-increase/>
- İleri, E., & Koçar, G. (2013). Effects of antioxidant additives on engine performance and exhaust emissions of a diesel engine fueled with canola oil methyl ester-diesel blend. *Energy Conversion and Management*, 76, 145-154.
- Ithnin, A. M., Noge, H., Abdul Kadir, H., & Jazair, W. (2014). An overview of utilizing water-in-diesel emulsion fuel in diesel engine and its potential research study. *Journal of the Energy Institute* 87(4), 273-288.
- Jaichandar, S., & Annamalai, K. (2013). The status of biodiesel as an alternative fuel for diesel engine—an overview. *Journal of Sustainable Energy & Environment*, 2(2), 71-75.
- Jain, S., & Sharma, M. P. (2010). Stability of biodiesel and its blends: a review. *Renewable and Sustainable energy reviews*, 14(2), 667-678.
- Jain, S., & Sharma, M. P. (2012). Application of thermogravimetric analysis for thermal stability of Jatropha curcas biodiesel. *Fuel*, 93, 252-257.
- Janaun, J., & Ellis, N. (2010). Perspectives on biodiesel as a sustainable fuel. *Renewable and Sustainable Energy Reviews*, 14(4), 1312-1320.

- Jayadas, N. H., Prabhakaran Nair, K., & G, A. (2007). Tribological evaluation of coconut oil as an environment-friendly lubricant. *Tribology International*, 40(2), 350-354.
- Jayed, M., Masjuki, H., Kalam, M., Mahlia, T., Husnawan, M., & Liaquat, A. (2011). Prospects of dedicated biodiesel engine vehicles in Malaysia and Indonesia. *Renewable and Sustainable energy reviews*, 15(1), 220-235.
- Jiang, X., Naoko E., & Zhong Z. (2011). Fuel properties of bio-diesel mixture characterized by TG, FTIR and ¹H-NMR. *Korean Journal of Chemical Engineering*, 28(1), 133-137.
- Joshi, G., Lamba, B. Y., Rawat, D. S., Mallik, S., & Murthy, K. (2013). Evaluation of additive effects on oxidation stability of Jatropha Caurcas biodiesel blends with conventional diesel sold at retail outlets. *Industrial & Engineering Chemistry Research*, 52(22), 7586-7592.
- Kannan, G. R., & Anand, R. (2011). Experimental investigation on diesel engine with diestrol–water micro emulsions. *Energy*, 36(3), 1680-1687.
- Kannan, T. K., & Gounder, M. R. (2011). Thevetia peruviana biodiesel emulsion used as a fuel in a single cylinder diesel engine reduces nox and smoke. *Thermal science*, 15, 1185-1191.
- Kato, K., & Adachi, K. (2001). Wear mechanisms. *Modern tribology handbook*, 1, 273-300.
- Kerihuel, A., Senthil Kumar, M., Bellettre, J., & Tazerout, M. (2005). Use of animal fats as CI engine fuel by making stable emulsions with water and methanol. *Fuel*, 84(12–13), 1713-1716.
- Khatri, K. K., Sharma, D., Soni, S., & Tanwar, D. (2010). Experimental investigation of CI engine operated micro-trigeneration system. *Applied Thermal Engineering*, 30(11), 1505-1509.
- Khond, V. W., & Kriplani, V. M. (2016). Effect of nanofluid additives on performances and emissions of emulsified diesel and biodiesel fueled stationary CI engine: A comprehensive review. *Renewable and Sustainable Energy Reviews*, 59, 1338-1348.
- Knothe, G., & Steidley, K. R. (2005). Kinematic viscosity of biodiesel fuel components and related compounds. Influence of compound structure and comparison to petrodiesel fuel components. *Fuel*, 84(9), 1059-1065.
- Knothe, G. (2007). Some aspects of biodiesel oxidative stability. *Fuel Processing Technology*, 88(7), 669-677.
- Koc, A. B., & Abdullah, M. (2013). Performance and NOx emissions of a diesel engine fueled with biodiesel-diesel-water nanoemulsions. *Fuel Processing Technology*, 109(0), 70-77.

- Kovaříková, I., Szewczykova, B., Blaškoviš, P., Hodúlová, E., & Lechovič, E. (2009). Study and characteristic of abrasive wear mechanisms. *Materials Science and Technology [online]*.-ISSN, 1335-9053.
- Kuchler, M., & Linnér, B.-O. (2012). Challenging the food vs. fuel dilemma: Genealogical analysis of the biofuel discourse pursued by international organizations. *Food Policy*, 37(5), 581-588.
- Kwanchareon, P., Luengnaruemitchai, A., & Jai-In, S. (2007). Solubility of a diesel–biodiesel–ethanol blend, its fuel properties, and its emission characteristics from diesel engine. *Fuel*, 86(7–8), 1053-1061.
- Labeckas, G., Slavinskas, S., & Mažeika, M. (2014). The effect of ethanol–diesel–biodiesel blends on combustion, performance and emissions of a direct injection diesel engine. *Energy Conversion and Management*, 79(0), 698-720.
- Laugel, C., Baillet, A., Youenang Piemi, M. P., Marty, J. P., & Ferrier, D. (1998). Oil-water-oil multiple emulsions for prolonged delivery of hydrocortisone after topical application: Comparison with simple emulsions. *International Journal of Pharmaceutics*, 160(1), 109-117.
- Lif, A., & Holmberg, K. (2006). Water-in-diesel emulsions and related systems. *Advances in colloid and interface science*, 123, 231-239.
- Lin, C.-Y., & Chen, L.-W. (2006). Emulsification characteristics of three- and two-phase emulsions prepared by the ultrasonic emulsification method. *Fuel Processing Technology*, 87(4), 309-317.
- Lin, C.-Y., & Lin, H.-A. (2007). Engine performance and emission characteristics of a three-phase emulsion of biodiesel produced by peroxidation. *Fuel Processing Technology*, 88(1), 35-41.
- Lin, C.-Y., & Lin, H.-A. (2008). Effects of NO_x-inhibitor agent on fuel properties of three-phase biodiesel emulsions. *Fuel Processing Technology*, 89(11), 1237-1242.
- Lin, C.-Y., & Wang, K.-H. (2003). The fuel properties of three-phase emulsions as an alternative fuel for diesel engines. *Fuel*, 82(11), 1367-1375.
- Lin, C. Y., & Lin, S. A. (2007). Effects of emulsification variables on fuel properties of two- and three-phase biodiesel emulsions. *Fuel*, 86(1-2), 210-217.
- Lin, Y.-S., & Lin, H.-P. (2011). Spray characteristics of emulsified castor biodiesel on engine emissions and deposit formation. *Renewable Energy*, 36(12), 3507-3516.
- Liu, Y., Erdemir, A., & Meletis, E. I. (1996). A study of the wear mechanism of diamond-like carbon films. *Surface and Coatings Technology*, 82(1–2), 48-56.
- M Senthil Kumar, J. B., M Tazerout. (2009). The use of biofuel emulsions as fuel for diesel engines: A review. *Journal of power and energy*, 223.

- Madankar, C. S., Dalai, A. K., & Naik, S. N. (2013). Green synthesis of biolubricant base stock from canola oil. *Industrial Crops and Products*, 44, 139-144.
- Moilanen, D. E., Fenn, E. E., Wong, D., & Fayer, M. D. (2009). Water Dynamics at the Interface in AOT Reverse Micelles. *The Journal of Physical Chemistry B*, 113(25), 8560-8568.
- Mosarof, M. H., Kalam, M. A., Masjuki, H. H., Alabdulkarem, A., Ashraful, A. M., Arslan, A., . . . Monirul, I. M. (2016). Optimization of performance, emission, friction and wear characteristics of palm and Calophyllum inophyllum biodiesel blends. *Energy Conversion and Management*, 118, 119-134.
- Moser, B. R. (2011). Biodiesel production, properties, and feedstocks *Biofuels* (pp. 285-347): Springer.
- Motorship, T. (2014). Emulsion trial could spark new interest, from <http://www.motorship.com/news101/fuels-and-oils/emulsion-trial-could-spark-new-interest>
- Nadeem, M., Rangkuti, C., Anuar, K., Haq, M. R. U., Tan, I. B., & Shah, S. S. (2006). Diesel engine performance and emission evaluation using emulsified fuels stabilized by conventional and gemini surfactants. *Fuel*, 85(14-15), 2111-2119.
- Nesterenko, A., Drelich, A., Lu, H., Clause, D., & Pezron, I. (2014). Influence of a mixed particle/surfactant emulsifier system on water-in-oil emulsion stability. *Colloids and Surfaces A: Physicochemical and Engineering Aspects*, 457(0), 49-57.
- Nohava, J., Morstein, M., & Dessarzin, P. (2016). High temperature tribological behavior of advanced hard coatings for cutting tools, from <http://www.anton-paar.com/mx-es/productos/applications/high-temperature-tribological-behavior-of-advanced-hard-coatings-for-cutting-tools/>
- Ong, H., Mahlia, T., & Masjuki, H. (2011). A review on energy scenario and sustainable energy in Malaysia. *Renewable and Sustainable Energy Reviews*, 15(1), 639-647.
- Opawale, F. O., & Burgess, D. J. (1998). Influence of Interfacial Properties of Lipophilic Surfactants on Water-in-Oil Emulsion Stability. *Journal of Colloid and Interface Science*, 197(1), 142-150.
- OPEC. (2016). OPEC share of world crude oil reserves, 2016. Retrived from http://www.opec.org/opec_web/en/data_graphs/330.htm
- Optical microscope. (2008), from https://www.cs.mcgill.ca/~rwest/link-suggestion/wpcd_2008-09_augmented/wp/o/Optical_microscope.htm
- Owen, N. A., Inderwildi, O. R., & King, D. A. (2010). The status of conventional world oil reserves—Hype or cause for concern? *Energy Policy*, 38(8), 4743-4749.
- Özcanlı, M., Keskin, A., & Aydın, K. (2011). Biodiesel production from terebinth (pistacia terebinthus) oil and its usage in diesel engine. *International Journal of Green Energy*, 8(5), 518-528.

- Palash, S. M., Kalam, M. A., Masjuki, H. H., Masum, B. M., Rizwanul Fattah, I. M., & Mofijur, M. (2013). Impacts of biodiesel combustion on NO_x emissions and their reduction approaches. *Renewable and Sustainable Energy Reviews*, 23(0), 473-490.
- Palash, S. M., Kalam, M. A., Masjuki, H. H., Masum, B. M., & Sanjid, A. (2014). Impacts of NO_x reducing antioxidant additive on performance and emissions of a multi-cylinder diesel engine fueled with Jatropha biodiesel blends. *Energy Conversion and Management*, 77, 577-585.
- Petroleum, B. (2011). Statistical Review of World Energy 2011.
- Phan, A. N., & Phan, T. M. (2008). Biodiesel production from waste cooking oils. *Fuel*, 87(17-18), 3490-3496.
- Plantation, S. D. (2014). Palm oil facts & figures. Retrieved from http://www.simedarby.com/upload/Palm_Oil_Facts_and_Figures.pdf
- Porras, M., Solans, C., González, C., & Gutiérrez, J. M. (2008). Properties of water-in-oil (W/O) nano-emulsions prepared by a low-energy emulsification method. *Colloids and Surfaces A: Physicochemical and Engineering Aspects*, 324(1-3), 181-188.
- Prakash, R., Singh, R. K., & Murugan, S. (2015) Experimental studies on combustion, performance and emission characteristics of diesel engine using different biodiesel bio oil emulsions. *Journal of the Energy Institute*, 88(1) 64-75.
- Qi, D. H., Chen, H., Lee, C. F., Geng, L. M., & Bian, Y. Z. (2010). Experimental studies of a naturally aspirated, DI diesel engine fuelled with ethanol-biodiesel-water microemulsions. *Energy and Fuels*, 24(1), 652-663.
- Qi, D. H., Chen, H., Matthews, R. D., & Bian, Y. Z. (2010). Combustion and emission characteristics of ethanol-biodiesel-water micro-emulsions used in a direct injection compression ignition engine. *Fuel*, 89(5), 958-964.
- Raheman, H., & Kumari, S. (2014). Combustion characteristics and emissions of a compression ignition engine using emulsified jatropha biodiesel blend. *Biosystems Engineering*, 123(0), 29-39.
- Reham, S. S., Masjuki, H. H., Kalam, M. A., Shancita, I., Fattah, I. M. R., & Ruhul, A. M. (2015). Study on stability, fuel properties, engine combustion, performance and emission characteristics of biofuel emulsion. *Renewable and Sustainable Energy Reviews*, 52, 1566-1579.
- Rizwanul Fattah, I. M., Kalam, M. A., Masjuki, H. H., & Wakil, M. A. (2014). Biodiesel production, characterization, engine performance, and emission characteristics of Malaysian Alexandrian laurel oil. [10.1039/C3RA47954D]. *RSC Advances*, 4(34), 17787-17796.
- Rizwanul Fattah, I. M., Masjuki, H. H., Kalam, M. A., Mofijur, M., & Abedin, M. J. (2014). Effect of antioxidant on the performance and emission characteristics of

a diesel engine fueled with palm biodiesel blends. *Energy Conversion and Management*, 79, 265-272.

Rizwanul Fattah, I. M., Masjuki, H. H., Liaquat, A. M., Ramli, R., Kalam, M. A., & Riazuddin, V. N. (2013). Impact of various biodiesel fuels obtained from edible and non-edible oils on engine exhaust gas and noise emissions. *Renewable and Sustainable Energy Reviews*, 18(0), 552-567.

Roila Awang, & May, C. Y. (2008). Water in oil emulsion of palm biodiesel. *Journal of Oil Palm Research* 20, 571-576.

Sadhik Basha, J., & Anand, R. B. (2014). Performance, emission and combustion characteristics of a diesel engine using Carbon Nanotubes blended Jatropa Methyl Ester Emulsions. *Alexandria Engineering Journal*, 53(2), 259-273.

SCIENTIFIC, T. NMR Application: Process Control, from <https://www.thermoscientific.com/en/about-us/general-landing-page/nmr-process-control.html>

Senthil Kumar, M., & Jaikumar, M. (2014). A comprehensive study on performance, emission and combustion behavior of a compression ignition engine fuelled with WCO (waste cooking oil) emulsion as fuel. *Journal of the Energy Institute*, 87(3), 263-271.

Shahir, S. A., Masjuki, H. H., Kalam, M. A., Imran, A., Fattah, I. M. R., & Sanjid, A. (2014). Feasibility of diesel-biodiesel-ethanol/bioethanol blend as existing CI engine fuel: An assessment of properties, material compatibility, safety and combustion. *Renewable and Sustainable Energy Reviews*, 32, 379-395.

Society of Petroleum & Engineers. (2014, 22 october 2014). Stability of oil emulsions, from http://petrowiki.org/Stability_of_oil_emulsions

Sperring, T., & Nowell, T. (2005). SYCLOPS—a qualitative debris classification system developed for RAF early failure detection centres. *Tribology international*, 38(10), 898-903.

Stachowiak, G. W. (2006). *Wear: materials, mechanisms and practice*: John Wiley & Sons.

Staniford, S. (2008). Powering Civilization to 2050, Retrived from <http://www.theoil drum.com/node/3540>

Syahrullail, S., Wira, J. Y., Nik, W. B. W., & Fawwaz, W. N. (2013). Friction Characteristics of RBD Palm Olein Using Four-Ball Tribotester. *Applied Mechanics and Materials*, 315, 936-940.

Tariq, M., Ali, S., Ahmad, F., Ahmad, M., Zafar, M., Khalid, N., & Khan, M. A. (2011). Identification, FT-IR, NMR (1H and 13C) and GC/MS studies of fatty acid methyl esters in biodiesel from rocket seed oil. *Fuel Processing Technology*, 92(3), 336-341.

- Tesfa, B., Mishra, R., Gu, F., & Ball, A. (2012). Water injection effects on the performance and emission characteristics of a CI engine operating with biodiesel. *Renewable Energy*, *37*(1), 333-344.
- United States Department of Agriculture, U. (2007). Indonesia: palm oil production prospects continue to grow.
- Ushikubo, F. Y., & Cunha, R. L. (2014). Stability mechanisms of liquid water-in-oil emulsions. *Food Hydrocolloids*, *34*(0), 145-153.
- Wan Nik, W. B., Ani, F. N., & Masjuki, H. H. (2005). Thermal stability evaluation of palm oil as energy transport media. *Energy Conversion and Management*, *46*(13-14), 2198-2215.
- Wang, R., Zhou, W.-W., Hanna, M. A., Zhang, Y.-P., Bhadury, P. S., Wang, Y., . . . Yang, S. (2012). Biodiesel preparation, optimization, and fuel properties from non-edible feedstock, *Datura stramonium* L. *Fuel*, *91*(1), 182-186.
- Wu, J.-M., Lin, S.-J., Yeh, J.-W., Chen, S.-K., Huang, Y.-S., & Chen, H.-C. (2006). Adhesive wear behavior of Al x CoCrCuFeNi high-entropy alloys as a function of aluminum content. *Wear*, *261*(5), 513-519.
- Xin, J., Imahara, H., & Saka, S. (2008). Oxidation stability of biodiesel fuel as prepared by supercritical methanol. *Fuel*, *87*(10-11), 1807-1813.
- Xue, J., Grift, T. E., & Hansen, A. C. (2011). Effect of biodiesel on engine performances and emissions. *Renewable and Sustainable Energy Reviews*, *15*(2), 1098-1116.
- Züge, L. C. B., Haminiuk, C. W. I., Maciel, G. M., Silveira, J. L. M., & Scheer, A. d. P. (2013). Catastrophic inversion and rheological behavior in soy lecithin and Tween 80 based food emulsions. *Journal of Food Engineering*, *116*(1), 72-77.

LIST OF PUBLICATIONS AND PAPERS PRESENTED

Journal Article

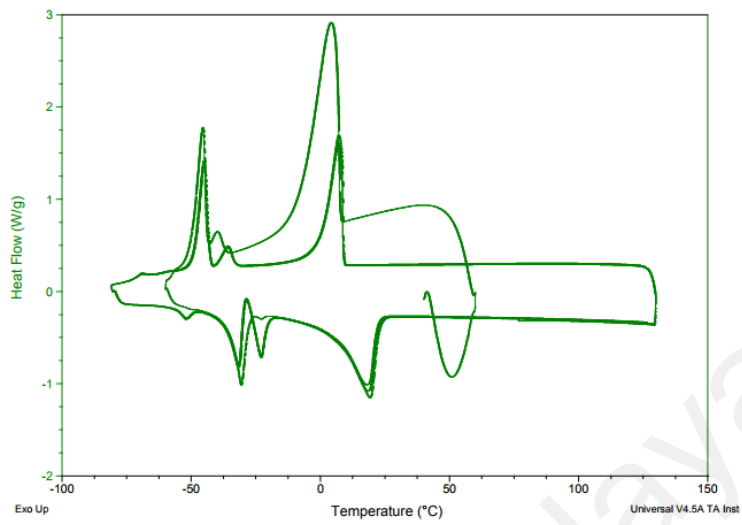
S.S. Reham, H.H. Masjuki, M.A. Kalam, I. Shancita, I.M. Rizwanul Fattah, A.M. Ruhul, “Study on stability, fuel properties, engine combustion, performance and emission characteristics of biofuel emulsion” *Renewable and Sustainable Energy Reviews*, 52 (2015) 1566–1579. [ISI Indexed, Q1]

S.S. Reham, H.H. Masjuki, M.A. Kalam, I. Shancita, M.H. Mosarof, A.M. Ruhul, “Improvement of oxidation and thermal stability of Palm oil methyl ester through emulsification and assessment of its lubrication characteristics” *Biofuel Research Journal* (Under Revision) [ISI Indexed]

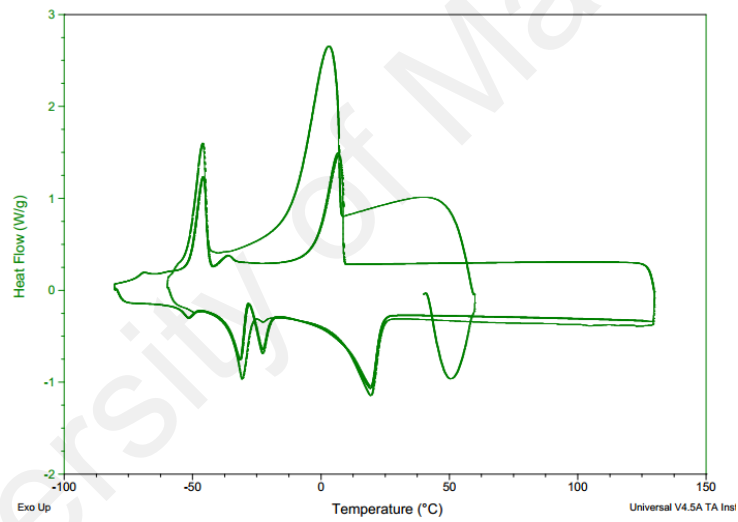
Conference Article

S.S. Reham, H.H. Masjuki, M.A. Kalam, “FTIR and ¹H NMR analysis of water emulsified Palm biodiesel with Span 80” *International Journal of Engineering Technology, Management and Applied Sciences*, September 2015, Volume 3, Special Issue, ISSN 2349-4476.

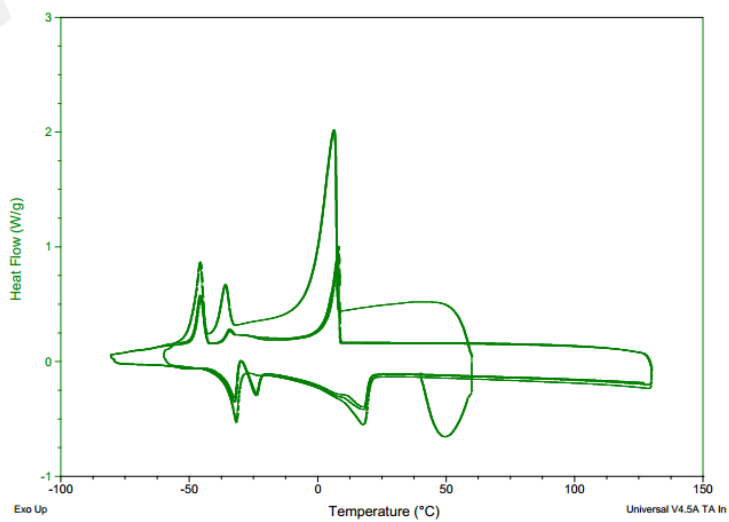
APPENDIX



(a)



(b)



(c)

Figure: Heat flow graph of (a) MTX-1, (b) MTX-2 and (c) MTX-3